

Instituto Tecnológico y de Estudios Superiores de Monterrey

Campus Monterrey

School of Engineering and Sciences



Study on the Convective Heat Transfer Behaviour of  
Laminar Nanofluids Flow

A dissertation presented by

Ramón Ramírez Tijerina

Submitted to the  
School of Engineering and Sciences  
in partial fulfillment of the requirements for the degree of

Doctor of Philosophy

In

Engineering Science

Monterrey Nuevo León, May 15<sup>th</sup>, 2019

## **Dedication**

This thesis work is dedicated to my wife, Claudia, who has been a constant source of support and encouragement during the challenges of graduate school and life. I am truly thankful for having you in my life. This work is also dedicated to my parents, Ramon and Isabel, who have always loved me unconditionally and whose good examples have taught me to work hard for the things that I aspire to achieve.

## **Acknowledgements**

I would like to express my sincere gratitude to Dr. Carlos Iván Rivera Solorio for his guidance and assistance in this thesis. The technical discussions with Prof. Rivera were always insightful, and I will always be indebted with him for all the knowledge that he shared with me during the past few years. His prompt response and availability despite his constantly busy schedule were truly appreciated. Prof. Carlos is much more than an advisor for me as he always helped me in all the technical and non-technical issues during this work. His encouragement and efforts led this thesis to successful completion in a timely fashion.

I am also thankful to the Tecnológico de Monterrey for covering the full extent of the tuition during the course of this program and for giving the opportunity to continue learning and developing my research skills and knowledge.

# Study on the Convective Heat Transfer Behaviour of Laminar Nanofluids Flow

By

Ramón Ramírez Tijerina

## Abstract

Nanofluids are engineered colloids of nanoparticles dispersed homogeneously within base fluids. The term nanofluids refers to a mixture composed of a continuous phase, usually a saturated liquid, and a dispersed phase constituted of extremely fine metallic particles of size below 100 nm called nanoparticles. Due to the presence of nanoparticles, the thermophysical and transport properties of base fluids are subject to change. The nanofluids are considered the next-generation heat transfer fluids because of the new possibilities compared to pure fluids. Existing technologies for industrial applications, such as: microelectronics, vehicle thermal management (engine cooling) and heat exchangers seem to be insufficient and nanofluids, as reported in several studies, might offer a better alternative for proper heat transfer.

The main purpose of this study is to investigate numerically the potential for replacing nanofluids in a single-phase flow for a conventional straight tube and a straight microtube under the constant temperature and constant heat flux conditions, separately. Nanofluids with a wide range of process parameters had been studied by varying three different types of base fluids including water, ethylene glycol and oil with five different types of nanoparticles viz.  $\text{Al}_2\text{O}_3$ ,  $\text{TiO}_2$ ,  $\text{CuO}$ ,  $\text{SiO}_2$  and  $\text{ZnO}$ . During the present investigation, six different combinations of the geometries, based fluids and nanoparticle concentrations were considered.

The thermophysical properties of the nanofluids were obtained from the literature. The mathematical modeling was done using single-phase approach (SPH) where the flow was assumed as a steady incompressible flow and the continuity, momentum and energy equations are solved using the effective properties of the nanofluids.

In addition to the single-phase model (SPH), the single-phase dispersion model (SPD) was also used for effectiveness of the computed results. The governing equations of mass, momentum and energy were solved using finite volume approach/method.

To ensure the accuracy and consistency of computational results, various uniform grids were tested. An extensive number of numerical simulations were performed to determine the Nusselt number (Nu) of laminar nanofluids. For validation purposes, the present results of the Nusselt number were compared with the literature computational and experimental results. The results showed that the Nusselt number increases with increase in Reynolds number (Re) for all the nanofluids considered. In the case of the straight tube with  $\phi_b = 4\%$ , the Nu increases 16% for Al<sub>2</sub>O<sub>3</sub>-water as compared to water, 12% for Al<sub>2</sub>O<sub>3</sub>-EG as compared to EG and 8% for Al<sub>2</sub>O<sub>3</sub>-oil as compared to oil. The investigation concludes with the proposition of heat transfer correlations for the flow of nanofluids in conventional straight tube and straight microtube over a wide range of process conditions:  $25 < \text{Re} < 1500$ ,  $0 < \phi_b < 10$ ,  $6 < \text{Pr} < 500$ .

## List of Figures

Figure 1. Visual example of a nanofluid .....	21
Figure 2. Density for Al <sub>2</sub> O <sub>3</sub> /water nanofluids: (a) comparison between theoretical models and experimental data, (b) effective density as a function of temperature. ....	26
Figure 3. Specific heat of Al <sub>2</sub> O <sub>3</sub> - water nanofluid at room temperature. ....	27
Figure 4. Factor influencing nanofluid forced convection heat transfer performance. ...	35
Figure 5. Experimental rig used by Haghghi et al. [26]. ....	48
Figure 6. Experimental rig with TC, thermocouple; HD, hydrodynamically. ....	49
Figure 7. Computational domain: straight tube and straight microtube. ....	58
Figure 8. Comparison of Nu for Al <sub>2</sub> O <sub>3</sub> -water nanofluid (a) constant heat flux condition at $\phi_b = 1\%$ . (b) constant wall temperature condition at $\phi_b = 4\%$ . ....	65
Figure 9. Effect of nanoparticle concentration in tube flow: (a) fluid temperature profiles at tube exit, (b) axial development of wall temperature. ....	67
Figure 10. Effect of nanoparticle concentration in tube flow: (a) axial development of $T_m$ , (b) axial development of wall temperatures. ....	67
Figure 11. Comparison of Nu for an Al <sub>2</sub> O <sub>3</sub> -water nanofluid at $\phi_b = 0\%$ , 1% and 4%. ...	69
Figure 12. Comparison of Nu for water-based nanofluids at $\phi_b = 4\%$ . ....	69
Figure 13. Effect of nanoparticle concentration in tube flow: axial development of wall temperatures. ....	70
Figure 14. Comparison of Nu for Al <sub>2</sub> O <sub>3</sub> -water, Al <sub>2</sub> O <sub>3</sub> -EG and Al <sub>2</sub> O <sub>3</sub> -turbine oil at $\phi_b = 4\%$ . ....	72
Figure 15. Proposed correlation vs computed results and experiments of Nu in a straight tube. ....	72
Figure 16. Effect of nanoparticle concentration in tube flow: axial development of wall and $T_m$ . ....	73
Figure 17. Comparison of Nu for Al <sub>2</sub> O <sub>3</sub> -water, TiO <sub>2</sub> -water, CuO-water, SiO <sub>2</sub> -water and ZnO-water and at $\phi_b = 4\%$ . ....	74
Figure 18. Comparison of Nu for Al <sub>2</sub> O <sub>3</sub> -water, Al <sub>2</sub> O <sub>3</sub> -EG and Al <sub>2</sub> O <sub>3</sub> -turbine oil at $\phi_b = 4\%$ . ....	75
Figure 19. Proposed correlation vs computed results and experiments of Nu in a straight tube. ....	75

Figure 20. Comparison of Nu with literature: Al <sub>2</sub> O <sub>3</sub> -water nanofluid at $\phi_b = 4\%$ .....	76
Figure 21. Effect of nanoparticle concentration in tube flow: (a) axial development of wall temperatures, (b) fluid mean temperatures for Al <sub>2</sub> O <sub>3</sub> -water. ....	77
Figure 22. Comparison of Nu for water-based nanofluids at $\phi_b = 4\%$ .....	78
Figure 23. Comparison of Nu for Al <sub>2</sub> O <sub>3</sub> -water, Al <sub>2</sub> O <sub>3</sub> -EG and Al <sub>2</sub> O <sub>3</sub> -turbine oil at $\phi_b = 4\%$ .....	78
Figure 24. Proposed correlation vs computed results and experiments of Nu in a straight tube. ....	79
Figure 25. Comparison of Nu with literature: Al <sub>2</sub> O <sub>3</sub> -water nanofluid at $\phi_b = 4\%$ for SPH and SPD.....	80

## List of Tables

Table 1. The different nanofluids and their process parameters. ....	16
Table 2. Nusselt number for a pipe with constant heat flux. ....	34
Table 3. Details of the Test Sections.....	50
Table 4. Details of the geometries considered for the numerical study. ....	58
Table 5. Thermophysical properties equations of nanoparticles. ....	60
Table 6. Thermophysical properties of different base liquid types.....	61
Table 7. Thermophysical properties of different nanoparticles types. ....	62
Table 8. Mesh Independency Test. ....	62
Table 9. Cases considered to determine the HTC enhancement of nanofluids.....	64
Table B. 1 Experimental and numerical studies for forced convective heat transfer of nanofluids for laminar flow.....	85



# Table of Contents

<b>Abstract</b> .....	<b>6</b>
<b>List of Figures</b> .....	<b>8</b>
<b>List of Tables</b> .....	<b>10</b>
<b>1 Introduction</b> .....	<b>13</b>
1.1 Motivation .....	13
1.2 Problem Statement and Context.....	14
1.3 Research Question.....	17
1.4 Solution overview .....	18
1.5 Main Contributions.....	19
1.6 Thesis Organization.....	19
<b>2 Literature Review</b> .....	<b>21</b>
2.1 Nanofluids and their significance .....	21
2.2 Thermophysical properties of nanofluids .....	23
2.3 Preparation of Nanofluids .....	30
2.4 Laminar Flow Heat Transfer .....	32
2.5 Nanofluid Forced Convection .....	34
2.6 Conventional straight tube .....	41
2.7 Micro straight tube .....	42
2.8 Heat Exchangers using Nanofluids.....	45
2.9 Nanofluids Experimental Setup .....	46
2.10 Heat Transfer Enhancement.....	50
2.11 Modeling Convection in Nanofluids .....	54
<b>3 Mathematical Formulation</b> .....	<b>57</b>
3.1 Governing Equations .....	57
3.2 Geometrical Configuration .....	58
3.2 Thermophysical Properties .....	59
3.3 Grid Independence Test .....	62

<b>4 Results and Discussion</b> .....	<b>64</b>
4.1 Case 1: Water nanofluid in st. tube with constant heat flux using SPH .....	65
4.2 Case 2: Ethylene glycol nanofluid in st. tube with constant heat flux using SPH..	70
4.3 Case 3: Turbine oil nanofluid in st. tube with constant heat flux using SPH .....	70
4.4 Case 4: Water nanofluid in st. tube with constant wall temperature using SPH....	73
4.5 Case 5: Water-based nanofluid in st. microtube with constant heat flux using SPH .....	76
4.6 Case 6: Water-based nanofluid in st. tube with constant heat flux using SPD.....	79
<b>5 Conclusions &amp; Recommendations</b> .....	<b>81</b>
5.1 Conclusions .....	81
5.2 Main contributions .....	82
5.3 Recommendations.....	83
<b>Appendix A</b> .....	<b>84</b>
<b>Appendix B</b> .....	<b>85</b>
<b>Bibliography</b> .....	<b>87</b>
<b>Curriculum Vitae</b> .....	<b>94</b>

# CHAPTER

## 1 Introduction

### 1.1 Motivation

Nanofluids are now considered the next generation heat transfer fluids because they offer exciting new possibilities to enhance heat transfer performance compared to pure liquids. They are expected to have superior properties compared to conventional heat transfer fluids, as well as fluids containing micro-sized metallic particles. Also, nanofluids can improve abrasion-related properties as compared to the conventional solid/fluid mixtures. Successful employment of nanofluids will support the current trend toward component miniaturization by enabling the design of smaller and lighter heat exchanger systems. However, the development of nanofluids is still hindered by several factors such as: lack of agreement between results, poor characterization of suspensions, and lack of theoretical understanding of the mechanisms. Suspended nanoparticles in various base fluids can alter the fluid flow and heat transfer characteristics, therefore, studies need to be carried out before a wide application for nanofluids can be found.

The main purpose of this thesis is to investigate if the addition of nanoparticles can enhance the heat transfer performance of commonly used fluids (e.g. water, ethylene glycol and oil) over a wide range of process conditions ( $25 < \text{Re} < 1500$ ,  $0 < \phi_b < 10$ ,  $6 < \text{Pr} < 500$ ). Heat transfer in nanofluids has been investigated for almost twenty years, but results are still confusing which led to a controversial issue, namely, whether or not the anomalous convective heat transfer enhancement is possible in nanofluid convective heat transfer. One of the aims of this study is to review previous investigations reports in the literature and propose a wider range of process conditions to enable the comparison of convective heat transfer of nanofluids to that of their base fluids.

In order to compare the thermal performance of nanofluids to base fluids, the thermo-physical and transport properties of nanofluids must be investigated. Furthermore, it is crucial to be confident that the accuracy of the computations is acceptable to be able to propose the desired correlations. It is also important to suggest several analytic methods for evaluating the heat transfer performance of the nanofluids.

Moreover, it is essential to determine a simple calculation to estimate the enhancement of the heat transfer of nanofluids to base fluids to promote the use and application of nanofluids over the base fluids.

## **1.2 Problem Statement and Context**

Industrial process involving heating and cooling of fluids inside the conduits of all sorts are widespread and represent some of the most common and important processes found in engineering today. Indeed, in thermal engineering, forced convection is probably the most effective and widely used means to transfer heat [1]. Applications include various types of heat exchangers, heating and cooling units, and a multitude of other flow-induced heat transfer situations. As heat transfer is related to the fluid's thermophysical properties, the possibilities of increasing a fluid's thermal conductivity is quite appealing.

Increased demands for improved cooling and heat dissipation technologies as well as the growing need for more compact and energy-efficient thermal management systems are continuously challenging engineers to come up with innovative solutions. Nanofluids studies revealed that the use of suspensions containing nanoscale particles as heat transfer mediums were very promising [2]. In essence, high-performance coolants could provide more compact, energy efficient heat management systems and provide more efficient localized cooling. Although effective thermal conductivity enhancement is very promising, it is certainly not the only factor weighing in on a nanofluid's potential as a heat transfer medium. Other important factors include other thermophysical properties such as viscosity and specific heat, as well as flow-related parameters and considerations such as nanofluid stability, and flow conditions [3]. From this perspective, the interrelated factors influencing forced convection heat transfer performance can be quite complex. It become clear that an increase in fluid thermal conductivity is not a guarantee of increased performance in a forced convection application.

Convective heat transfer can be passively enhanced by changing flow geometry, boundary conditions, or fluid thermophysical properties. A way of improving the thermal conductivity of the fluid is to suspend small solid particles within it. This idea of adding solids to create a liquid mixture is not new.

Maxwell, at the end of nineteenth century, demonstrated the possibility of increasing the thermal conductivity of a liquid mixture by adding solid nanoparticles to it. At that time, because of the limited manufacturing capabilities, only particles with dimensions on the order of micrometers could be produced. But suspensions with these types of particles caused abrasion of the tube wall and a substantial increase in the wall shear stress. It is also known, that Maxwell theory quite underestimates the magnitude of the thermal conductivity enhancement of metal nanofluids but still, is widely use in the literature for comparison purposes.

Today, it is possible to readily manufacture nanometer-sized particles and is disperse them within a base fluid such as water. These types of suspensions have been referred to as nanofluids. The term nanofluids refers to a mixture composed of a continuous phase, usually a saturated liquid, and a dispersed phase constituted of extremely fine metallic particles of a size below 100 nm called nanoparticles. As it is known, nanofluids are considered the next generation heat transfer fluids because of the new possibilities such as: more heat transfer surface between particle and fluids, reduced pumping power to achieve equivalent heat transfer intensification and others when they are compared to pure liquid. It has been shown that the thermal properties of a nanofluid appear to be higher than those of the base fluid. Hence, nanofluids appear to be an interesting alternative for advanced thermal applications for nanoscale heat transfer [4].

Three possible approaches have been pursued for the study of nanofluids: experimental, theoretical and numerical. Although the number of experimental, theoretical and numerical work has been constantly increasing since 1993, few works have been published on theoretical or numerical studies of nanofluids [5-15]. The current lack of understanding of the basic mechanism of energy transport at the nanoscale makes the published theoretical works on nanofluids extremely case dependent. In other words, researchers have been fitting data to experiments, rather than obtaining fundamental understanding. Numerical works aimed at basic understanding are sporadic in the literature and the only papers published recently oversimplify the physics [16].

Alumina ( $\text{Al}_2\text{O}_3$ ) nanofluids are the most common nanofluids used by researchers and they have been widely used for both experimental and numerical work [17-26]. Wen and Ding [17] were the first researchers that developed a series of experiments using alumina/water nanofluids in a circular tube with 970 mm length and 6.4 mm of outer diameter. They observed that the convective heat transfer improved in the laminar flow regime by using  $\text{Al}_2\text{O}_3$  nanoparticles. After Wen and Ding, several researchers have continued to work in understanding the heat transfer improvements in nanofluids for a laminar flow regime not only for  $\text{Al}_2\text{O}_3$  nanoparticles but for many other nonmetallic solids such as: Copper oxide ( $\text{CuO}$ ), Silicon Oxide ( $\text{SiO}_2$ ), Titania ( $\text{TiO}_2$ ), Zinc Oxide ( $\text{ZnO}$ ).

A summary of the studies, both experimental and theoretical, that have been conducted to calculate the convective heat transfer coefficient of the nanofluids flow in straight tube under laminar flow condition are shown in Table 1. Three process parameters were selected:  $Re$ ,  $Pr$  and  $\phi_b$ , to determine what has been studied previously and for comparison purposes. These parameters were selected on the potential of the nanofluids for their practical applications as studied by previous authors. The highest Prandtl number ( $Pr$ ) and volume fraction of nanoparticles were 753 and  $\phi_b=10\%$ , respectively.

From the literature review performed during this study, it was conclusive that there are only few investigations of the heat transfer coefficient of nanofluids flow in straight tube with a wider range of nanoparticles and particle concentrations.

**Table 1.** The different nanofluids and their process parameters.

Author	Nanofluids	Re	Pr	$\phi_b$
Wen and Ding [17]	$\text{Al}_2\text{O}_3$ -water	500–2100	6–12	0.6–1.6
Maïga et al. [18]	$\text{Al}_2\text{O}_3$ -water, $\text{Al}_2\text{O}_3$ -EG	250–1000	6–753	0–10.0
Heris et al. [19]	$\text{CuO}$ -water, $\text{Al}_2\text{O}_3$ -water	650–2050	6–12	0.2–3.0
	$\text{CuO}$ -, $\text{TiO}_2$ -, $\text{Al}_2\text{O}_3$ - Turbine Oil	650–2050	350–500	0–1
Anoop et al. [20]	$\text{Al}_2\text{O}_3$ -water	500–2000	6–12	1.0–6.0
Hwang et al. [21]	$\text{Al}_2\text{O}_3$ -water	500–800	6–12	0.01–0.3
Davarnejad et al. [22]	$\text{Al}_2\text{O}_3$ -water	420–990	6–12	0.5–2.5
Kim et al. [23]	$\text{Al}_2\text{O}_3$ -water	800–2400	6–12	0–3
Rea et al. [24]	$\text{Al}_2\text{O}_3$ -water, $\text{ZrO}_2$ -water	10–2000	6–12	0–6.0
Purohit et al. [25]	$\text{Al}_2\text{O}_3$ -, $\text{ZrO}_2$ -, $\text{TiO}_2$ -water	1150–1900	6–12	0.5–2
Haghighi et al. [26]	$\text{Al}_2\text{O}_3$ -, $\text{ZrO}_2$ -, $\text{TiO}_2$ -water	10–2300	6–12	2.3

This is mainly because the experimental analysis can be complicated due to time and cost for the wider range of the design parameters. A considerable amount of research has been done on nanofluids over the past decade, the conclusions on their behavior, characteristics, and performances remain somewhat controversial. There is still lack of consistency in experimental values found in the literature and challenges that need to be addressed and overcome before this new field of study can be fully established. It is imperative to conduct more investigations to properly quantify the effects of nanoparticles in heat transfer enhancement.

Therefore, in this study, the single-phase model was used for a wide range of nanofluid properties including three different base fluids with Prandtl numbers ranging from 6 – 500 and five different nanoparticles  $\text{Al}_2\text{O}_3$ ,  $\text{TiO}_2$ ,  $\text{CuO}$ ,  $\text{SiO}_2$  and  $\text{ZnO}$ . The wide range of fluid properties enables the evaluation of the performance of convective heat transfer in a large number of engineering applications that can benefit from a better understanding of the thermal enhancement of nanofluids. Furthermore, it is important to understand that the usefulness of nanofluids for heat transfer applications depends not only on the thermal conductivity but also on other transport properties, such as viscosity, and on thermodynamic properties, such as specific heat. The wide range of nanofluids properties will allow us to produce relevant Nu correlations, and more importantly, enable control by proper selection of particles and base fluids. It is important to highlight that, the nanoparticles diameter will also have an effect on the heat transfer coefficient, however, to simplify the numerical model and to speed up the computational time they were discarded in this study and proposed for future work.

### **1.3 Research Question**

To the best of our knowledge, a very limited number of research works have been found on nanofluids flow in a conventional straight tube and microtube covering a wide range of process conditions ( $25 < \text{Re} < 1500$ ,  $0 < \phi_p < 10$ ,  $6 < \text{Pr} < 500$ ). In addition to the process conditions, a wide range of process parameters such as geometries, base fluids and nanoparticle concentrations will help to determine what are the potential heat transfer improvements of the nanofluids considered in this study.

The investigation in this thesis will focus on answering:

- How the nanofluids can improve the heat transfer coefficient when they are exposed to different boundary conditions (constant heat flux and constant temperature)?
- Which mathematical model can be the more accurate to determine the heat transfer coefficient of the nanofluids: single-phase model or single-phase dispersion model?
- Which nanofluids from the fifteen different combinations between the three different type of base fluids including water, ethylene glycol and oil with five different nanoparticles viz.  $\text{Al}_2\text{O}_3$ ,  $\text{TiO}_2$ ,  $\text{CuO}$ ,  $\text{SiO}_2$  and  $\text{ZnO}$  shows a higher heat transfer coefficient enhancement?
- What is the heat transfer coefficient enhancement according to the different geometries (scale): conventional straight tube and straight microtube as they both have different industrial applications?

By answering this research questions it will possible to fulfill the general objective of this thesis that is to: determine the effect in the convective heat transfer coefficient in nanofluids for a straight tube and straight microtube for different nanoparticles ( $\text{Al}_2\text{O}_3$ ,  $\text{TiO}_2$ ,  $\text{CuO}$ ,  $\text{SiO}_2$  and  $\text{ZnO}$ ), base fluids (water, ethylene glycol and oil) and boundary conditions (uniform heat flux and uniform surface temperature) using single phase and single phase dispersion numerical models.

#### **1.4 Solution overview**

This investigation intends to create a step closer to build better heat exchangers systems by determining what is necessary to improve the heat transfer. This will be important in the near future as new and more effective heat exchangers are needed to improve the productivity and cost of the different industries where they are used. Through the development it will be possible to determine if the heat transfer coefficient is being improved when different boundary conditions are being applied.



To determine if the heat transfer can be improved different mathematical models will be used. The governing equations of mass, momentum and energy to be solved by using finite volume approach/method. The semi implicit method for pressure linked equations (SIMPLE) to be employed to couple pressure and velocity in equations. A second order upwind scheme to be employed for interpolating the parameters. A structure grid distribution to be used to discretize the computational domain. To ensure the accuracy and the consistency of computational results, various uniform grids to be tested.

From the computational results, the wall and fluid temperatures and the heat flux to be computed to calculate the convective heat transfer coefficient. Further the local and average heat transfer coefficient to be calculated together with the Nusselt number.

### **1.5 Main Contributions**

The main contributions of this investigations are the following:

- Heat transfer correlations for the flow of nanofluids in conventional straight tube and straight microtube over a wide range of process conditions ( $25 < Re < 1500$ ,  $0 < \phi_b < 10$ ,  $6 < Pr < 500$ ).
- Comparison between the single-phase model (SPH) and the single-phase dispersion model (SPD) to determine the effectiveness of the computed results.
- Identification of the Nusselt number improvements from three different type of based fluids including water, ethylene glycol and oil with five different type of nanoparticles viz.  $Al_2O_3$ ,  $TiO_2$ ,  $CuO$ ,  $SiO_2$  and  $ZnO$ .
- Demonstration that the addition of nanoparticles clearly showed an increase of the Nusselt number as compared to the base fluids.

### **1.6 Thesis Organization**

**Chapter 1** presents an introduction to the new generation heat transfer fluid known as nanofluid and how the use of nanofluid affects the heat transfer performance in engineering systems. Also, the problem statement and context, the research question and solution overview as well as the main contributions and the outline of this thesis is presented too.

**Chapter 2** presents a literature review on the nanofluids flow in a conventional straight tube and straight microtube under laminar flow. The significance, the thermophysical properties and the heat convection of the nanofluids is also mentioned.

**Chapter 3** presents the mathematical model namely single-phase (including dispersion model) to govern the steady incompressible fluid flow and heat transfer in a conventional straight tube and straight microtube. In addition, thermophysical properties of base fluids, nanofluids and nanoparticles are presented.

In **Chapter 4**, laminar forced convection was investigated for the flow of nanofluids in conventional straight tube and straight microtube under the constant temperature and constant heat flux conditions, separately. A wide range of the process parameters has been studied by varying three different type of base fluids including water, ethylene glycol and oil with five different type of nanoparticles viz.  $\text{Al}_2\text{O}_3$ ,  $\text{TiO}_2$ ,  $\text{CuO}$ ,  $\text{SiO}_2$  and  $\text{ZnO}$ . Heat transfer correlations are proposed for the flow of nanofluids over a wide range of process conditions ( $25 < \text{Re} < 1500$ ,  $0 < \phi_b < 10$ ,  $6 < \text{Pr} < 500$ ).

**Chapter 5** provides conclusions of Numerical Study of Heat Transfer Enhancement for Laminar Nanofluids Flow.

# Chapter

## 2 Literature Review

At present times, industrial technology related to heat transfer has considerably been concerned to design new tools and research to apply nanofluids is in progress in order to enhance the heat transfer rate. Therefore, the focus of concentration is on the experimental and numerical studies conducted in laminar to turbulent nanofluids flow with single phase, Eulerian-Eulerian mixture model and Eulerian-Lagrangian discrete phase approaches. In this chapter, several experimental and numerical research works related to nanofluids flow in a conventional straight tube and straight microtube have been presented and discussed.

### 2.1 Nanofluids and their significance

Dilute dispersions of nanoparticles (like metals, metal oxides, carbides, carbon nanotubes, etc.) with loading less than 10 vol% in conventional heat transfer fluids (like water, ethylene glycol/water, oil, etc.) are defined as nanofluids [1-2]. This new class of heat transfer fluids has been suggested to be used for high heat flux applications. Figure 1 shows a visual example of Nanofluid including  $\text{Al}_2\text{O}_3$  nanoparticles dispersed in a base fluid (water).

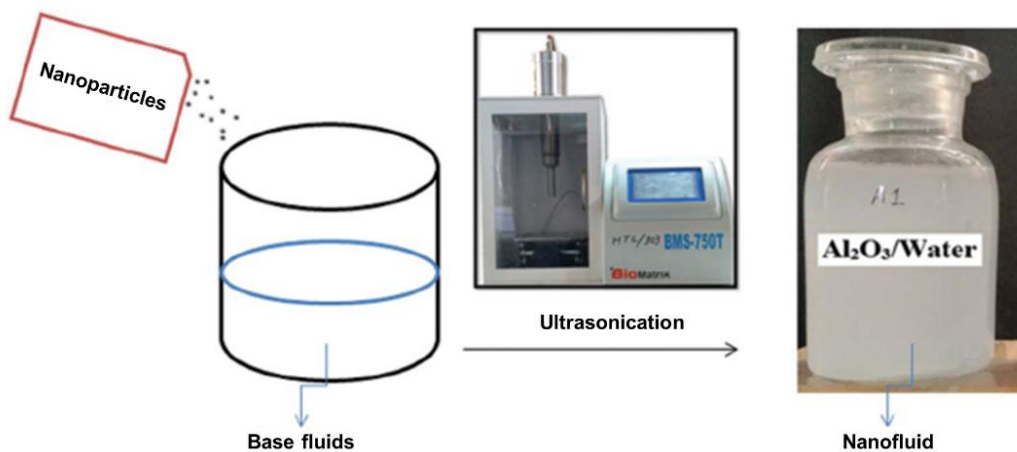


**Figure 1.** Visual example of a nanofluid.

Nanofluids are considered the next-generation heat transfer fluids because of the new possibilities (i.e. more heat transfer surface between particles and fluids, reduced pumping power to achieve equivalent heat transfer intensification, etc.) compare to pure liquids, however, this idea is not new. Maxwell, at the end of nineteenth century, demonstrated the possibility of increasing the thermal conductivity of a liquid mixture by adding solid particles to it.

At that time, because of the limited manufacturing capabilities, only particles with dimensions on the order of micrometers could be produced. But suspensions with these types of particles caused abrasion of the tube wall and a substantial increase in the wall shear stress.

Today, it is possible to readily manufacture nanometer-sized particles and disperse them within a base fluid such as water. These types of suspensions have been referred to as nanofluids. It appears that Choi from Argonne Laboratory coined this word in 1995. Attempts have been made to explain the physical reasons for thermal enhancement in nanofluids, still there are many inconsistencies. There are at least four reasons of why a definitive theory on nanofluids does not exist [3]:

- The thermal behaviour is too different from solid-solid composites or standard solid-liquid suspensions.
- The thermal transport in nanofluids, besides being surprisingly efficiently compared to standard solid-liquid suspensions, depends on nontraditional variables, such as particle size, shape, and surface treatment.
- The understanding of the physics behind nanofluids requires a multidisciplinary approach.
- Difficulty related to multiscale issues. Nanofluids involve at least four scales: the molecular scale, the microscale, the mesoscale, and the macroscale. The main difficulty is in the methods chosen to correlate and optimize the interplay among these scales.

There are large number of engineering applications that can benefit from a better understanding of the thermal conductivity enhancement of nanofluids. One example is ionic liquids, which are salts that are liquid at room temperature. However, ionic liquids do not have a very high thermal conductivity compared to water, and if this could be improved by the addition of nanoparticles, the liquid would be better suited for heat transfer applications such as in absorption refrigeration or cooling circuits [4].

Liquid cooling with high thermal conductivity fluids would also address many other heat dissipation problems. For instance, microelectro - mechanical system generate large quantities of heat during operation and require high-performance coolants to mitigate the large heat flux. Such a system requires precise temperature control, and a higher conductive fluid would allow for more efficient heat transfer control. There are also many everyday applications in which nanofluids could be suitable for, such as in the automotive industry. The high thermal conductivity enhancement observed in ethylene glycol-based nanofluids suggests that this common antifreeze could have better performance simply with a nanoparticle suspension.

## **2.2 Thermophysical properties of nanofluids**

In order to calculate the expected Nusselt numbers of nanofluids, their thermophysical properties need to be determined. These properties are thermal conductivity, viscosity, specific heat and density. Thermal conductivity is the most widely used studied thermophysical property of nanofluids.

Since the first experimental evidence [5] with alumina nanoparticles in water, the curiosity and interest in the scientific community has grown. Many different materials have been tested for nanoparticles with different based fluids, and the results are astonishingly different for various combinations. The vast majority of thermal conductivity experiments in nanofluids are conducted using the transient hot wire method. Other common techniques in the literature include the temperature oscillation method and the optical beam deflection technique [6], the 3- $\omega$  method [7], and the thermal wave technique [8].

Even though the literature on heat convection in nanofluids is limited compared to that in thermal conductivity, the results and approaches in the field are quite diverse and worth mentioning. In the first place, it is important to understand that whether nanofluids are Newtonian or shear thinning is relevant. This question was addressed by the first work ever done on heat convection in nanofluids in 1998 by Pak and Cho [9]. They reported that the nanofluids behaved as Newtonian when 13- and 27-nm nanoparticles of  $\text{Al}_2\text{O}_3$  and  $\text{TiO}_2$  were suspended in water, but only very low particle volume fractions. Shear-thinning behavior was, however, detected with an increase of particle volume fraction.

Pak and Cho also observed a large increase in the viscosity of both nanofluids and showed that this behavior was not predicted by standard empirical models for suspensions viscosities. The shear thinning behaviour sometimes reported in the literature is mainly attributed to three factors: the effective particle loading, the range of shear rate and the viscosity of the based fluids. Such non-Newtonian behavior can be characterized by a characteristic shear rate that decreases with increasing nanoparticle loading, increasing viscosity of the base fluid, or increasing nanoparticle cluster size.

Literature on experimental specific heats of nanofluids is very limited and has just lately been getting more attention. Namburu et al. [10] reported that several ethylene glycol-based nanofluids exhibit lower specific heat than their respective base fluids. Similarly, Bergman [11] reported experimental evidences that a water-alumina nanofluid appeared to have enhanced thermal conductivity but lower specific heat, relative to the base fluid. Shin and Banerjee [12] proposed three independent thermal transport mechanisms to explain the unusual enhancement of the specific heat they observed:

- **Mode 1:** The specific heat is enhanced due to higher specific surface energy of the surface atoms of the nanoparticles, compared to the bulk material. The surface energy is higher because of the low vibrational frequency and higher amplitudes of the vibrations at the surface of the nanoparticles.
- **Mode 2:** The enhancement of the specific heat can also be due to additional thermal storage mechanisms generated by interfacial interactions between nanoparticles and the liquid molecules, which act as virtual spring-mass systems.

This interfacial effect is present due to the extremely high specific surface area of the nanoparticles.

- **Mode 3:** A third mechanism potentially involved is liquid layering. Solid-like liquid layers adhering to the nanoparticles are more likely to have an enhanced specific heat due to a shorter intermolecular mean free path compared to the bulk fluid.

### Properties of Nanofluid

The properties of stable nanofluids with metals such as copper, silver, gold and oxides, namely Al<sub>2</sub>O<sub>3</sub>, CuO, TiO<sub>2</sub>, SiO<sub>2</sub>, Zn and ZrO<sub>2</sub>, in water and ethylene glycol are widely investigated because of their potential as heat transfer fluid with applications for thermal energy transfer in automotive, solar, and cooling electronic appliances. Studies are undertaken to determine ways to stabilize nanofluids from agglomeration for long term applications. The thermophysical properties of nanofluids which are important for application involving single phase convective heat transfer are viscosity, thermal conductivity, specific heat and density [13-29].

### Density

The density of nanofluid is based on the physical principle of the mixture rule. As such it can be represented as:

$$\rho_{eff} = \left(\frac{m}{V}\right)_{eff} = \frac{m_b + m_p}{V_b + V_p} = \frac{\rho_b V_b + \rho_p V_p}{V_b + V_p} = (1 - \phi_b)\rho_b + \phi_b\rho_p \quad (1)$$

where  $f$  and  $p$  refer to the fluid and nanoparticle respectively and  $\phi_b = V_p / (V_f + V_p)$  is the volume fraction of the nanoparticles.

To examine the validity of the effective density equation, two available studies, Pak et al. [30] and Ho et al. [31] conducted various experimental studies to measure the density of Al<sub>2</sub>O<sub>3</sub>/water nanofluids at room temperature as it can be seen in the Figure 2.

The Figure 2a shows an agreement between the experimental results and the predictions using the equation. The physical properties and different temperatures are important for calculations purposes and reflect the real conditions of the nanofluids. Results from the effective density of Al<sub>2</sub>O<sub>3</sub>/water nanofluids are shown in Figure 2a.

Ho et al. [31] measured the density of Al<sub>2</sub>O<sub>3</sub>/water nanofluid at different temperatures and nanoparticle fractions. Using the experimental data his study, Khanafer et al. [33] developed the density as a function of temperature and volume fraction. Figure 2b shows that the rate decrease of the effective density of Al<sub>2</sub>O<sub>3</sub>/water nanofluid with increasing temperature is insignificant. This is due the fact that the density of the Al<sub>2</sub>O<sub>3</sub> nanoparticles is less sensitive to the temperature when compared to the density of water.

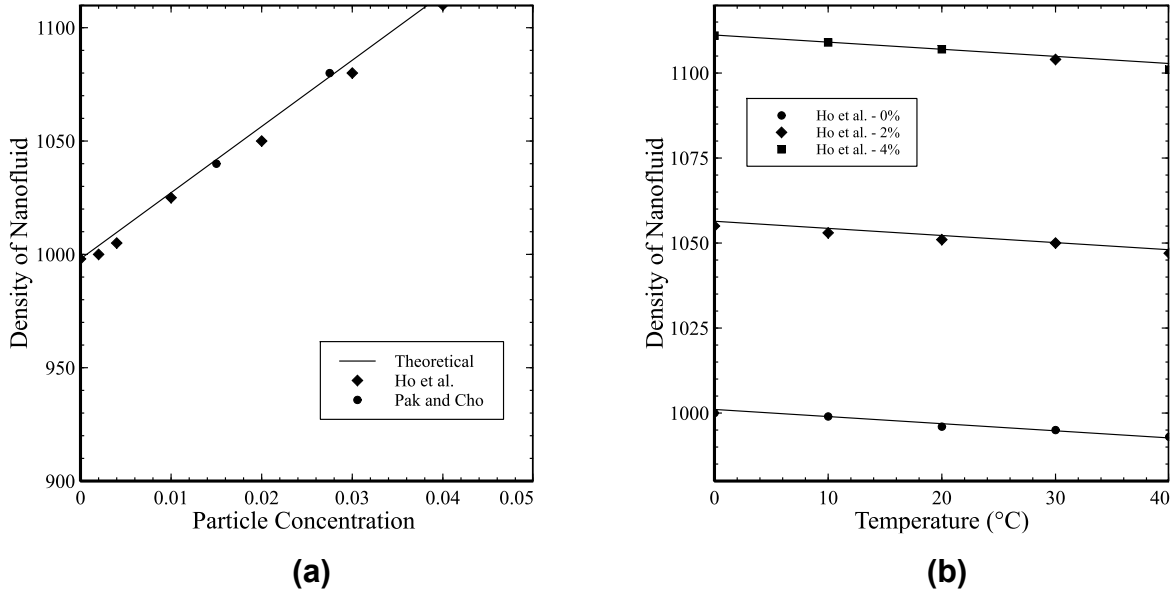


**Figure 2.** Density for Al<sub>2</sub>O<sub>3</sub>/water nanofluids: (a) comparison between theoretical models and experimental data, (b) effective density as a function of temperature.

## Heat Capacity

The specific heat of nanofluid can be determined by assuming thermal equilibrium between the nanoparticles and the based fluid phase as follows:

$$(\rho c)_{eff} = \rho_{eff} \left( \frac{Q}{m\Delta T} \right)_{eff} = \rho_{eff} \frac{Q_f + Q_p}{(m_f + m_p)\Delta T} = \frac{(mc)_f \Delta T + (mc)_p \Delta T}{(m_f + m_p)\Delta T} = \rho_{eff} \frac{(\rho c)_f V_f + (\rho c)_p V_p}{(\rho_f V_f + \rho_p V_p)} \rightarrow c_{eff} = \frac{(1 - \phi_b)\rho_f c_f + \phi_p \rho_p c_p}{\rho_{eff}} \quad (2)$$



where  $\rho_p$  is the density of the nanoparticle,  $\rho_f$  is the density of the base fluid,  $\rho_{eff}$  is the density of the nanofluid, and  $c_p$  and  $c_f$  are the heat capacities of the nanoparticle and the base fluid, respectively.

In the literature, several authors Das et al. [32], Jang et al. [68], Gosselin et al. [69] and Lee et al. [70] preferred to use a simpler expression given as:

$$c_{eff} = (1 - \phi_p)c_f + \phi_p c_p \quad (3)$$

Figure 3 shows a comparison of the specific heat of Al<sub>2</sub>O<sub>3</sub>- water nanofluid at room temperature using both equations with the experimental data of Zhou et al. [71] for various volume fractions. The Figure 3 shows that the specific heat of the nanofluid based on the models decreases with an increase in the volume fraction of nanoparticles. The experimental results were compared with the predictions obtained from the models. Model 1 compares very well with the experimental data.

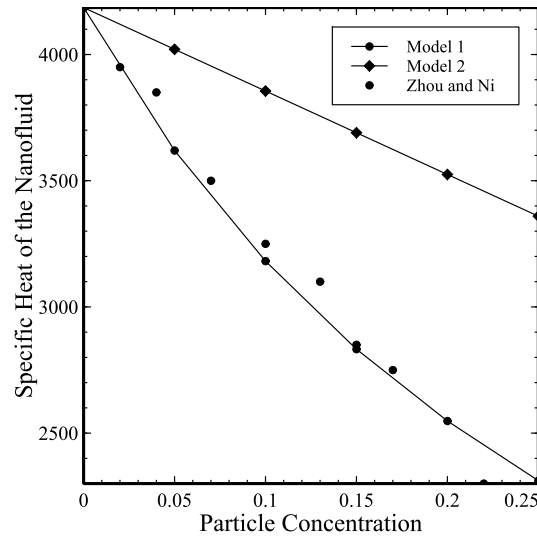


**Figure 3.** Specific heat of Al<sub>2</sub>O<sub>3</sub>- water nanofluid at room temperature.

## Viscosity

Different models of viscosity have been used by researchers to model the effective viscosity of nanofluid as a function of volume fraction. Brinkman et al. [34] presented a viscosity correlation that extended Einstein's equation to concentrated suspensions:

$$\mu_{eff} = \frac{1}{(1-\phi_p)^{2.5}} = (1 + 2.5\phi_p + 4.375\phi_p^2 + \dots)\mu_f \quad (4)$$

The effect of Brownian motion on the effective viscosity in a suspension of rigid spherical particles was studied by Batchelor et al. [36].

For isotropic structure of suspension, the effective viscosity was given by:

$$\mu_{eff} = (1 + 2.5\phi_p + 6.2\phi_p^2)\mu_f \quad (5)$$

Lundgren et al. [35] proposed the viscosity model under the form of a Taylor series in  $\phi_p$ :

$$\mu_{eff} = \frac{1}{1-2.5\phi_p} \mu_f = (1 + 2.5\phi_p + 6.25\phi_p^2 + O(\phi_p^3))\mu_f \quad (6)$$

All the above correlations were developed to relative viscosity as a function of volume fraction only; without any temperature dependence considerations. It should be mentioned that there are few studies in the literature associated with the effect of temperature on the viscosity of nanofluids.

For example, Nguyen et al. [72] investigated experimentally the influence of the temperature on the dynamic viscosities of two water-based nanofluid, namely Al<sub>2</sub>O<sub>3</sub>-water and CuO-water mixtures. The following formulas:

$$\mu_{eff} = (1.125 - 0.0007xT)\mu_f; \phi_p = 1\% \quad (7)$$

$$\mu_{eff} = (2.1275 - 0.0215xT + 0.0002xT^2)\mu_f; \phi_p = 4\% \quad (8)$$

## Thermal conductivity

Several ranges of experimental and theoretical studies can be found in the literature to model thermal conductivity of nanofluids. Published results in the literature present neither agreement about the mechanisms for heat transfer nor a unified possible explanation regarding the rather larger discrepancies in the results even for the same base fluid and nanoparticles size. Currently, there are no theoretical results available in the literature that predicts accurately the thermal conductivity of nanofluids. The existing results were generally based on the definition of the effective thermal conductivity of a two - components mixtures as presented by Hamilton et al. [37]:

$$k_{eff} = \frac{k_f(1-\phi_p)\left(\frac{dT}{dx}\right)_f + k_p\phi_p\left(\frac{dT}{dx}\right)_p}{\phi_p\left(\frac{dT}{dx}\right)_p + (1-\phi_p)\left(\frac{dT}{dx}\right)_f} \quad (9)$$

where  $(dT/dx)_f$  is the temperature gradient within the fluid and  $(dT/dx)_p$  is the temperature gradient through the particle.

The Maxwell model [38] was one the first models proposed for solid-liquid mixture with relatively large particles. It was based on the solution of heat conduction equation through a stationary suspension of spheres. The effective thermal conductivity is given by:

$$k_{eff} = \frac{k_p + 2k_f + 2\phi_p(k_p - k_f)}{k_p + 2k_f - \phi_p(k_p - k_f)} k_f = k_f + \frac{3\phi_p(k_p - k_f)}{k_p + 2k_f - \phi_p(k_p - k_f)} \quad (10)$$

where  $k_p$  is the thermal conductivity of the particles,  $k_f$  is the fluid conductivity,  $\phi_p$  is the volume fraction of the suspended particles.

A general correlation for  $Al_2O_3$  was presented by Khanafer et al. [33] using the available experimental data at various temperatures, nanoparticle's diameter, and volume fraction:

$$\frac{k_{eff}}{k_f} = 0.9843 + 0.398\phi_p^{0.7383} \left(\frac{1}{d_p}\right)^{0.2246} \left(\frac{\mu_{eff}(T)}{\mu_f(T)}\right)^{0.0235} - 0.39517\frac{\phi_p}{T} + 34.034\frac{\phi_p^2}{T^2}; 0 \leq \phi_p \leq 10\%, 20^\circ C \leq T \leq 70^\circ C, 11 \text{ nm} \leq d \leq 150 \text{ nm} \quad (11)$$

### 2.3 Preparation of Nanofluids

Preparation of nanofluids is the first key step in experimental studies with nanofluids. Nanofluids are not simply liquid-solid mixtures. Some special requirements are essential e.g. even and stable suspension, durable suspension, negligible agglomeration of particles, no chemical change of the fluid, etc. Nanofluids are produced by dispersing nanometer-scale solid particles into base liquids such as water, ethylene glycol (EG), oils, etc. In the synthesis of nanofluids, agglomeration is a major problem.

There are mainly two techniques used to produce nanofluids: the single-step and the two-step method. The single-step method direct evaporation approach was developed by Akoh et al. [73] and is called the VEROS (Vacuum Evaporation onto a Running Oil Substrate) technique. The original idea of this method was to produce nanoparticles, but it is difficult to subsequently separate the particles from the fluids to produce dry nanoparticles. A modified VEROS process was proposed by Wagener et al. [74].

They employed high pressure magnetron sputtering for the preparation of suspensions with metal nanoparticles such as Ag and Fe. Eastman et al. [75] developed a modified VEROS technique, in which Cu vapor is directly condensed into nanoparticles by contact with a flowing low-vapor-pressure liquid (EG).

Zhu et al. [76] presented a novel one-step chemical method for preparing copper nanofluids by reducing  $\text{CuSO}_4 \cdot 5\text{H}_2\text{O}$  with  $\text{NaH}_2\text{PO}_2 \cdot \text{H}_2\text{O}$  in ethylene glycol under microwave irradiation. Results showed that the addition of  $\text{NaH}_2\text{PO}_2 \cdot \text{H}_2\text{O}$  and the adoption of microwave irradiation are two significant factors which affect the reaction rate and the properties of Cu nanofluids. A vacuum-SANSS (submerged arc nanoparticle synthesis system) method has been deployed by Lo et al. [77] to prepare Cu-based nanofluids with different dielectric liquids such as de-ionized water, with 30%, 50% and 70% volume solutions of ethylene glycol and pure ethylene glycol. They found that the different morphologies, which are obtained, are mainly influenced and determined by the thermal conductivity of the dielectric liquids.  $\text{CuO}$ ,  $\text{Cu}_2\text{O}$  and Cu based nanofluids also can be prepared by this technique efficiently.

An advantage of the one-step technique is that nanoparticle agglomeration is minimized, while the disadvantage is that only low vapor pressure fluids are compatible with such a process.

The two-step method is extensively used in the synthesis of nanofluids considering the available commercial nanopowders supplied by several companies. In this method, nanoparticles were first produced and then dispersed the base fluids. Generally, ultrasonic equipment is used to intensively disperse the particles and reduce the agglomeration of particles. For example, Eastman et al. [75], Lee et al. [78] and Wang et al. [79] used this method to produce  $\text{Al}_2\text{O}_3$  nanofluids. Also, Murshed et al. [80] prepared  $\text{TiO}_2$  suspension in water using the two-step method. Other nanoparticles reported in the literature are gold (Au), silver (Ag), silica and carbon nanotubes. As compared to the single-step method, the two-step technique works well for oxide nanoparticles, while it is less successful with metallic particles.

Except for the use of ultrasonic equipment, some other techniques such as control of pH or addition of surface-active agents, are also used to attain stability of the suspension of the nanofluids against sedimentation. These methods change the surface properties of the suspended particles and thus suppress the tendency to form particle clusters. It should be noted that the selection of surfactants should depend mainly on the properties of the solutions and particles. Xuan and Li [81] chose salt and oleic acid as the dispersant to enhance the stability of transformer oil-Cu and water-Cu nanofluids, respectively. Oleic acid and CTAB surfactants were used by Murshed [80] to ensure better stability and proper dispersion of  $\text{TiO}_2$ -water nanofluids. Sodium dodecyl sulfate (SDS) was used by Hwang [82] during the preparation of water-based MWCNT nanofluids since the fibers are entangled in the aqueous suspension.

In general, methods such as change of pH value, addition of dispersant, and ultrasonic vibration aim at changing the surface properties of suspended particles and suppressing formation of particles cluster to obtain stable suspensions. However, the addition of dispersants can affect the heat transfer performance of the nanofluids, especially at high temperature.

## 2.4 Laminar Flow Heat Transfer

There are three different flow regimes of concern when working with fluids. These are turbulent, laminar, and transitional region. Transitional flow exists between laminar and turbulent regimes. Determination of the flow regime can be related to the Reynolds Number:

$$Re = \frac{\rho v D_{inner}}{\mu} \quad (12)$$

where  $\rho$  is the density,  $v$  is the mean flow velocity,  $\mu$  is the dynamic viscosity of the liquid, and  $D_{inner}$  is the inner tube diameter. Reynolds number is the ratio between inertia force and viscous force. When the Reynolds number is higher than 4800, the flow is turbulent. A Reynolds number between 2100 and 4800 corresponds to the transitional regime, i.e., the flow is in transition to the turbulent domain.

Flow is best described in streamlines. The streamlines of turbulent flow are chaotic in nature. With Reynold's experiment, it was discovered that turbulent flow has velocity fluctuations that causes the streamlines to move in an erratic matter.

Laminar flow, however, is very different. The streamline for laminar flow is steady and smooth. In fully-developed laminar flow the velocity profile is parabolic. The Reynolds number that is needed to maintain a laminar flow is normally under 2100. This occurs with the combination of high viscosity and low density, velocity, and inner tube diameter.

Heat transfer in laminar flow regime can be solved analytically as describe from many authors in the literature. There are two types of boundary conditions that lead to two differential solutions. The first one is a constant surface temperature. The analytical solution for constant surface temperature is derived from the differential energy equation:

$$\frac{\partial^2 t}{\partial r^2} + \frac{1}{r} \frac{\partial t}{\partial r} = \frac{u}{\alpha} \frac{\partial t}{\partial x} - \frac{\partial^2 t}{\partial x^2} \quad (13)$$

In this energy equation  $T$  represents the temperature;  $r$  is radius,  $u$  velocity,  $x$  distance, and  $\alpha$  the thermal diffusivity, which is defined as:

$$\alpha = \frac{k}{\rho C_p} \quad (14)$$

Equation 13 can be re-arranged with dimensionless variables:

$$\frac{\partial^2 \theta}{\partial^2 r^+} + \frac{1}{r^+} \frac{\partial \theta}{\partial r^+} = (1 - r^{+2}) \frac{\partial \theta}{\partial x^+} \quad (15)$$

Here  $\theta$  is the non-dimensionless temperature and  $x^+$  is the non-dimensionless distance. For a circular tube  $x^+$  is defined as:

$$x^+ = \frac{x/r_0}{RePr} \quad (16)$$

Equation 16 is solved using the boundary condition of constant surface temperature to give a formula in the following form:

$$Nu_x = \frac{\sum G_n \exp(-\lambda_n x^+)}{2 \sum (G_n / \lambda_n^2) \exp(-\lambda_n^2 x^+)} \quad (17)$$

At infinite distance, or fully developed laminar flow, Nu equals 4.36.

The second condition that leads to an analytical solution for Nusselt number is constant heat flux. Using equation 15 the boundary condition for constant heat flux is used which gives the following formula:

$$Nu_x = \left[ \frac{1}{Nu_\infty} - \frac{1}{2} \sum \frac{\exp(-\gamma_m^2 x^+)}{A_m \gamma_m^4} \right]^{-1} \quad (18)$$

The formula above gives rise to a table that is used to find the Nusselt number throughout the entire length of the pipe. The results are displayed in the Table 1.

**Table 2.** Nusselt number for a pipe with constant heat flux.

$X^+$	Nusselt Number
0	$\infty$
0.002	12
0.004	9.93
0.01	7.49
0.02	6.14
0.04	5.19
0.1	4.51
$\infty$	4.36

## 2.5 Nanofluid Forced Convection

Industrial process involving heating and cooling of fluids flowing inside the conduits of all sorts are widespread and represent some of the most common and important processes found in engineering today [83]. Indeed, in thermal engineering, forced convection is probably the most effective and widely used means to transfer heat.

As heat transfer is directly related to the fluid's thermophysical properties, the possibilities of increasing, in particular, a fluid's thermal conductivity is quite appealing. Although effective thermal conductivity enhancement is very promising, it is certainly not the only factor weighing in on a nanofluid's potential as a heat transfer medium. Other important factors include other thermophysical properties such as viscosity and specific heat, as well as flow-related parameters and considerations such as particle clustering and migration, nanofluid stability, and, of course, flow conditions. Furthermore, these factor are often interdependent as shown in Figure 4 [84].

As one can see, from this somewhat simplistic perspective, the interrelated factors influencing forced convection heat transfer performance can be quite complex. It becomes quite clear that an increase in fluid thermal conductivity is not a guarantee of increased performance in a forced convection application.

It is generally recognized that heat can be transferred via three distinct modes, that is, conduction, convection, and radiation. Convective heat transfer is the typical mode found in fluids.



In reality, convection is the combination of two distinct energy transfer mechanisms, specifically heat diffusion (or conduction) and advection (due to bulk fluid flow). Fluid motion results from either a density gradient (natural buoyancy forces) or a pressure difference. In the first case, the process is typically called “natural convection”. In the case of a fluid caused by a pressure gradient, the fluid motion normally results from external surface forces produced through pumping or blowing, or in another mechanically assisted manner. This is most often called “forced convection”. Of course, heat transmission in a fluid can be a combination of both natural and forced connection, which is referred to as “mixed convection”.

In any event, forced convection is a mode of heat transmission that is present in countless engineering processes, including various types of heat exchangers, fan-assisted cooling, impinging jets, and so on.

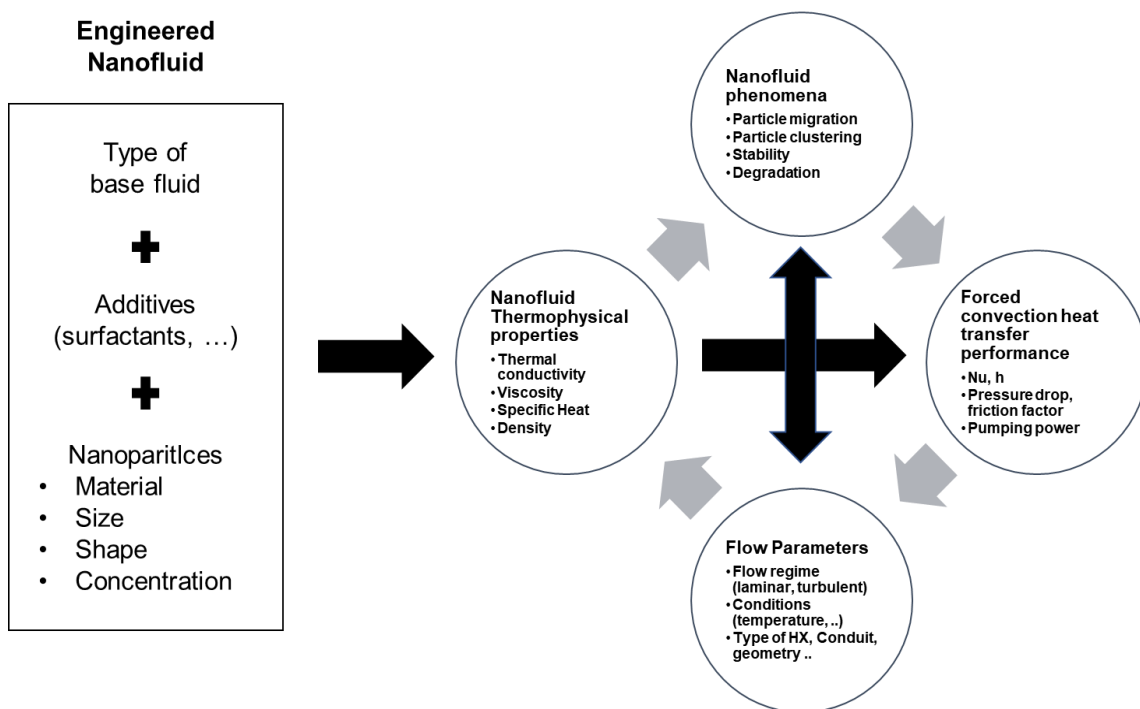


**Figure 4.** Factor influencing nanofluid forced convection heat transfer performance.

Generally speaking, the rate of heat transfer by convection between a surface and a fluid can be calculated from equation 19, initially proposed by Issac Newton (often called Newton's law of cooling):

$$\dot{Q}_c = \bar{h}_c A (T_w - T_{f,\infty}) = \bar{h}_c A \Delta T \quad (19)$$

where:

$\dot{Q}_c$  is the rate of heat transfer (W)

$\bar{h}_c$  is the average convective heat transfer coefficient (W/m<sup>2</sup>K)

A is the heat transfer surface area (m<sup>2</sup>)

$T_w$  and  $T_{f,\infty}$  are, respectively, the temperature at the surface of the solid and the fluid temperature at a reference location away from the surface (K)

By rewriting equation 19, the average heat transfer coefficient can be expressed as:

$$\bar{h}_c = \frac{\dot{Q}_c}{A(T_w - T_f)} = \frac{q_c''}{T_w - T_{f,\infty}} \quad (20)$$

where  $q_c''$  is the heat flux at the solid-fluid interface (W/m<sup>2</sup>). One should note that this equation represents the average heat transfer coefficient. Normally, the local value is determined, and the average value is then obtained through integration over the entire surface.

The convective heat transfer coefficient, unlike thermal conductivity, is not a physical property of the materials involved in the heat transfer process. Rather, the value of the convective heat transfer coefficient depends on a number of parameters such as flow velocity, temperature difference, and thermophysical properties of the fluid. As the value of these parameters normally are not constant over a surface or body, the numerical value of the heat transfer coefficient will therefore also vary along the surface.

In engineering applications, forced convection is typically used to increase the rate of heat exchange between a body and a fluid. As fluid temperature and velocity gradients are important factors in determining the heat transfer coefficient, an understanding of the underlying physics of fluid flow is essential in order to evaluate the heat transfer mechanisms in a fluid. The basic governing equations for fluid flow consist of a set of coupled partial derivative equations.

## **Governing Equations**

To derive the conservation equations for laminar flow, one usually uses a finite volume approach/method in which the rate of mass, momentum, and energy flowing into and out of the finite volume are accounted for. The finite volume method (FVM) is one of the most versatile discretization techniques used in Computational Fluid Dynamics (CFD). They have become popular as a result, primarily, of two advantages. First, they ensure that the discretization is conservative, i.e., mass, momentum and energy are conserved in a discrete sense. While this property can usually be obtained using a finite-difference formulation, it is obtained naturally from a finite-volume formulation. Second, finite-volume methods do not require a coordinate transformation in order to be applied on irregular meshes. As a result, they can be applied on unstructured meshes consisting of arbitrary polyhedral in three dimensions or arbitrary polygons in two dimensions. This increased flexibility can be used to great advantage in generating grids about arbitrary geometries.

Finite-volume methods are applied to the integral form of the governing equations. Based on the control volume formulation of analytical fluid dynamics, the first step in the FVM is to divide the domain into a number of control volumes (cells, elements) where the variable of interest is located at the centroid of the control volume. The next step is to integrate the differential form of the governing equations over each control volume. Interpolation profiles are then assumed in order to describe the variation of the concerned variable between cell centroids. The resulting equation is called the discretized or discretization equation. In this manner the discretization equation expresses the conservation principle for the variable inside the control volume.

The most compelling feature of the FVM is that the resulting solution satisfies the conservation quantities such as mass, momentum, energy, and species. The conservation momentum arises from applying Newton's second law to fluid motion, whereas the conservation of energy equation represents the first law of thermodynamics. Details of the development of these equations can be found in any standard fluid mechanics textbook. Assuming that the fluid is incompressible and Newtonian and that both compression work and viscous dissipation are assumed negligible in the energy equation, the general conservation equations for steady flow can be written in vector form as follows:

- Conservation of mass:  $\mathit{div}(\rho\vec{V}) = 0$  (21)

- Conservation of momentum:  $\mathit{div}(\rho\vec{V}\vec{V}) = -\mathit{grad} p + \mu\nabla^2\vec{V}$  (22)

- Conservation of energy:  $\mathit{div}(\rho\vec{V}C_pT) = \mathit{div}(k\mathit{grad}T)$  (23)

where:

$\rho$ ,  $\mu$ ,  $C_p$  and  $k$  are, respectively, the fluid density, viscosity, specific heat, and thermal conductivity of the considered fluid

$T$ ,  $p$ , and  $\vec{V}$  are, respectively, the temperature, pressure and velocity vector.

These equations are, except for highly simplified cases, impossible to solve analytically.

### **Force Convection Modeling**

From a theoretical standpoint, suspensions consisting of liquids and dispersed ultrafine particles (nanoparticles) represent a relatively new and technologically interesting sector. Developing new theories and models that would help predict nanofluid flow and heat transfer behaviors in engineering applications are complex challenges for researchers. Indeed, according to the literature, it appears quite difficult to formulate theories that could reasonably predict the flow and heat transfer of nanofluids by considering it as a multicomponent fluid. However, because a nanofluid is by nature a two-phase fluid, one could expect that it will most certainly possess some common features with conventional solid-fluid mixture behaviors.

Due to the minute size of the particles, certain interesting phenomena are believed to present in nanofluids but are not found in conventional mixtures containing large sized particles. These include thermal dispersion, intermolecular energy exchange, and liquid layering on the solid-liquid interface as well as phonon effects on the heat transport inside the particle itself. Generally speaking, two approaches to nanofluid forced convection modeling have been used and sometimes compared by various research groups. Essentially, some have treated nanofluids as single-phase fluids with “effective” thermophysical properties, whereas others have considered them as two component mixtures using various two-phase modeling approaches.

As most nanofluids considered for practical heat transfer applications are typically composed of ultrafine particles, it is conceivable that these may be easily fluidized. Consequently, by assuming negligible motion slip between the particles and the continuous phase and that thermal equilibrium conditions prevail between the two components, the nanofluid may then be considered as a conventional single-phase fluid, with effective thermophysical properties being the function of the properties of both constituents and their respective concentrations. If one views such an assumption as feasible, the classic theories developed for conventional single-phase fluids can then be applied to nanofluids as well. Thus, all the equations of conservation (mass, momentum, and energy) governing single-phase fluids can be directly extended and employed for nanofluids using effective thermophysical properties.

This approach has been used quite extensively in numerical research studies to date. Indeed, most of the early work on nanofluid forced convection used this approach. The most challenging aspect of using a single-phase fluid approach is specifying adequate effective thermophysical properties.

In the case of two-phase modeling, there are generally two approaches that can be used. Essentially, for mixtures containing low particle loadings, the Lagrangian-Eulerian approach is typically used. In this approach, the mixture is modeled using a Eulerian frame for the base fluid and a Lagrangian frame for the particles. For higher volume fractions of particles, the approach most often used is the Eulerian-Eulerian.

In the particular case of nanofluids, even for a small volume fraction, the number of particles will be extremely large due to their minute sizes. Therefore, the use of a Lagrangian-Eulerian approach becomes unpractical in a computational sense. As a result, Eulerian-Eulerian approaches are most often used for nanofluid two-phase flow modeling. Several Eulerian-Eulerian models exist, including the volume of fluid (VOF), the mixture model, and the Eulerian model. These are typically incorporated in popular commercially available CFD packages such as FLUENT. The VOF model was designed for two or more immiscible fluids, in which a single set of momentum equations is shared by all fluids (or phases). The volume fraction of each component is tracked over the entire computational domain by solving a continuity equation for the secondary phase (the sum of volume fractions of all phases equals unity).

The mixture model was specifically designed for two or more phases. This model is adequate for low volume fraction particulate flows. It solves the general conservation equations for the mixture as well as a volume fraction equation for the secondary phase. Finally, the Eulerian model is more complex multiphase model. Although the pressure is shared by all phases, it solves a separate set of momentum, continuity, and energy equations for each phase. Momentum exchange between the phase is dependent on the type of mixture being modeled.

Several research groups have made comparisons between single-phase and two-phase approaches. One of the first numerical studies to consider two-phase modeling for nanofluids was conducted by Behzadmehr et al. [49]. In their work, they considered turbulent forced convection of a water-1% volume copper nanofluid using a two-phase mixture model. For comparison purposes, they also considered the same problem using a single-phase approach with constant weighted average properties of the nanofluid. The results obtained by both modeling techniques were compared to available experimental data and the authors concluded that the mixture model was more precise than the single-phase model. In the two-phase approach the slip velocity between the fluid and particles might not be zero due to several factors such as gravity, friction between the fluid and solid particles, Brownian forces, Brownian diffusion, sedimentation and dispersion.

The two-phase approach provides a field description of the dynamics of each phase or, alternatively, the Lagrangian trajectories of individual particles couple with the Eulerian description of the fluid flow field.

## **2.6 Conventional straight tube**

Many researchers have investigated the effect of nanofluid in enhancing the heat transfer coefficient in straight tubes such as Bianco et al. [48]. In this study, they numerically investigated the developing laminar forced convection flow of a water- $\text{Al}_2\text{O}_3$  nanofluid in a circular tube submitted to a constant and uniform heat flux at the wall. The maximum difference in the average heat transfer coefficient between single and two-phase models resulted in 11%. The convective heat transfer coefficient for nanofluids is greater than that of the base liquid. Heat transfer enhancement increases with the particle volume concentration, but it is accompanied by increasing wall shear stress values.

The single-phase model with physical and thermal properties, all assumed to be constant with temperature was first employed by Maïga et al. [18]. The two-phase approach seems a better model to describe the nanofluid flow. A two-phase mixture model was applied to study the turbulent forced convection flow of a nanofluid in a uniformly heated tube by Behzadmehr [49-50]. More recently Namburu et al. [51] investigated turbulent convection flow of nanofluids inside a tube considering variable properties. In the investigation, they found that nanofluids containing smaller diameter nanoparticles have higher viscosity and Nusselt number. At a constant Reynolds number, Nusselt number increases by 35% for 6% CuO nanofluids over the base fluid. Ting et al. [52] investigated the forced convection heat transfer and flow characteristics of water-based  $\text{Al}_2\text{O}_3$  nanofluids inside a horizontal circular tube in the laminar flow regime under the constant wall temperature boundary condition. In their study, the heat transfer coefficient of the water-based nanofluid with 2 vol. %  $\text{Al}_2\text{O}_3$  nanoparticles is enhanced by 32% compared with that of pure water. Fard et al. [53] studied the laminar convective heat transfer of nanofluid in circular tube under constant wall temperature condition using CFD approach. Results show that the heat transfer coefficient clearly increases with Peclet number. Arzani et al. [54] conducted a numerical investigation into convective heat transfer of CuO-water based nanofluid in a pipe with return bend under laminar flow condition.

The results indicate that the increase in Reynolds number leads to the enhancement of average Nusselt number, and the increase in specific heat in the presence of the nanofluid results in improvement in heat transfer. Kristiawan et al. [55] studied numerically using a CFD code the laminar convective heat transfer of TiO<sub>2</sub>/water nanofluids through in tube. The results are reasonably well with Shah-London correlation for laminar flow.

## **2.7 Micro straight tube**

Over the last decade, micromachining technology has been increasingly used for the development of highly efficient cooling devices called heat sink because of its undeniable advantages such as less coolant demands and small dimensions. One of the most important micromachining technologies is micro channels.

Before proceeding with microchannel flow and heat transfer, it is appropriate to introduce a definition for the term “microchannel”. The scope of the term is among the topics of debate between researchers in the field. Obot [55] proposed a simple classification of the microchannel where the microchannel is based on the hydraulic diameter rather than the smallest channel dimension. Obot classified channels of hydraulic diameter under 1 mm as microchannels, which was also adopted by many other researchers. The higher volumetric heat transfer densities require advanced manufacturing techniques and lead to more complex manifold designs. Many of the same manufacturing techniques developed for the fabrication of electronic circuits are being used for the fabrication of compact heat exchangers.

Microchannel heat sinks constitute an innovative cooling technology for the removal of a large amount of heat through a small area. It is one of the potential alternatives for replacing conventional finned tube heat exchangers, mainly used in industries such as automobiles, air conditioning and refrigeration at present. The heat sink is usually made from a high thermal conductivity solid such as silicon or copper with the micro-channels fabricated into its surface by either precision machining or micro-fabrication technology.



A micro channel heat sink typically contains a large number of parallel micro channels. Coolant is forced to pass through these channels to carry away heat from a hot surface. In micro channel heat exchangers flow is typically laminar and heat transfer coefficients are proportional to velocity. Micro channel heat sinks provide very high surface area to volume ratio, large convective heat transfer coefficient, small mass and volume, and small coolant inventory. These attributes render these heat sinks very suitable for cooling devices such as high-performance microprocessors, laser diode arrays, radars, and high-energy-laser mirrors.

Some experimental and theoretical work on micro channel heat exchanger has been done in the last decade. Because nanoparticles are ultrafine, low-concentration nanofluids are expected to cause little penalty in pressure drop. Based on experimentally demonstrated augmentation in thermal conductivity, nanofluids are considered promising in enhancing forced convection heat transfer in microchannel related heat-generating microsystems. Experimental results showed that the Nusselt number increases with the Reynolds and Prandtl numbers as well as nanoparticles volume fraction. The enhancement is particularly significant in the entrance region, where local particle concentration was suggested to be the reason. Moreover, the ratio of convective heat transfer coefficients between the nanofluid and the base fluid was found to increase with the Peclet number as well as nanoparticles volume fraction.

The evaluation of nanofluids in microtube studies started with Vafaei et al. [56]. In the investigation, they reported that the heat transfer coefficient (HTC) depends on the mass flow rate and also on the concentration. Lee et al. [57] used  $\text{Al}_2\text{O}_3$ , CuO and Carbon nanotubes particles in water. These nanofluids presented an enhancement of 11.6% for CNT (0.2 vol%), 5.0% for  $\text{Al}_2\text{O}_3$  (3 vol%) and 13.3% for CuO (4 vol%).

Recently Haghghi et al. [26] performed an experiment for screening single phase laminar convective heat transfer with water and three different nanofluids. Results show enhancement in heat transfer of nanofluids only when compared at constant Reynolds number. Heris [58] conducted an experimental study of convective heat transfer of  $\text{Al}_2\text{O}_3$ -water nanofluid in a square duct under constant heat flux in laminar flow.

The convective heat transfer coefficient ration of the nanofluid to water was found to increase with the Peclet number up to 27.6% at 2.5% volume fraction. Heyhat [59] experimentally investigated the heat transfer coefficient and the friction factor of Al<sub>2</sub>O<sub>3</sub>-water nanofluid flowing in a horizontal tube under laminar flow conditions. They found that within volume fractions of 0.1% - 2%, the coefficient ration  $h_{nf}/h_{bf}$  increased with the Re and particle concentration.

It should be noted that the enhancement of the heat transfer coefficient is often found to be larger than that of the thermal conductivity for the same nanoparticles volume fraction. Particle migration effects, for example, shear stress, viscosity gradient, thermophoresis, and/or Brownian motion, have been proposed to account for the enhanced heat transfer performance of nanofluids over the base fluids in the laminar flow regime. It might lead to nonuniform thermal conductivity and viscosity profiles and reduce boundary layer thickness. The results obtained from different studies disagree and often lack physical explanations.

Daungthongsuk and Wongwises [60] discussed the method of calculation of heat transfer coefficient in case of micro channel heat exchanger using nanofluids. Numerical methods had also been used to analyze the performance of the behaviour and to design the micro channels heat exchanger.

In the numerical simulation of fluid flow and heat exchanger of nanofluids, the methods used in the literature can be categorized into three groups:

- Single-phase approach,
- Two-phase approach and,
- Lattice Boltzmann method (LBM).

In the single-phase approach, it is assumed that the suspended nanoparticles are in thermal equilibrium with the liquid phase and that the relative velocity between the two phases is negligible. The reason is that nanoparticles are so small that they follow the streamlines of the fluid exactly, making the mixture behave like a homogenous mixture. Thus, a set of governing equations for pure fluids can be used with the effective thermophysical properties of nanofluids replacing the fluid properties.

The single-phase approach is easy to implant and requires less computation time; the predicted results concerning convective heat transfer characteristics of nanofluids agree well with experiments. However, the results depend strongly on the selected thermophysical property models, especially those for thermal conductivity and viscosity.

To improve the single-phase model, some modifications have been applied to include the slip between the particles and the base fluid by adding a virtual term in the thermal conductivity expression. Also, solving the nanoparticles mass transfer equation together with the momentum and energy equations to account for nonuniform concentration distributions can also increase the accuracy. Nevertheless, the single-phase model provides acceptable results with low computational time requirements.

The two-phase models have been used only recently but have shown better accuracy than the single-phase model compared to experimental evidence. Also, the comparisons between different two-phase models favor the mixture model over the Eulerian two-phase model. Although the two-phase models are capable of capturing the nonuniform concentration fields, it should be noted that most studies assumed that the turbulence of the fluid phase is not directly affected by the presence of the nanoparticles phase.

## **2.8 Heat Exchangers using Nanofluids**

Heat exchangers are equipment being used for transfer heat between two or more fluids at different temperatures [61]. They are widely used in various fields, including power plants, automotive, space heating, refrigeration and air-conditioning systems, chemical plants, petrochemical processes, electronic cooling, and environmental engineering. Many heat transfer enhancement techniques have been developed for heat exchangers to improve their thermal efficiency by means of surface area enlargement and boundary layer modification. Conventional heat transfer fluids such as water, ethylene glycol, and engine oil have relatively low thermal conductivity values, which thus limit the heat transfer rates.

Due to recent progress in nanotechnology, thermal conductivity values can be increased by adding nanometer-sized structures (e.g., particles, fibers, tubes) in conventional heat transfer fluids to form the so-called nanofluids.

Heat transfer characteristics of nanofluids in straight tubes have been extensively studied as shown in reviews of Dalkilic et al. [62] and Hussein et al. [63]. However, no agreement on anomalous heat transfer enhancement has been achieved to date. Yang et al. [64] obtained exact solutions for fully developed laminar flow in straight channels and tubes and concluded that (1) the anomalous heat transfer enhancement was captured, especially for the case of titania-water nanofluids in a tube when the particle volume fractions are larger than 2% and (2) the maximum Nusselt number based on bulk mean nanofluid thermal conductivity is at  $N_{BT} = 0.5$ , although it became lower than that of the pure fluid at  $N_{BT} < 0.3$ . The parameter  $N_{BT}$  indicates the ration of Brownian and thermophoretic diffusivities.

So far, there have been few studies on heat transfer characteristics of nanofluids in complex geometries (e.g., microchannels, helically coiled tubes, enhanced tubes) and heat exchangers. Humenic and Humenic [65] reviewed about 20 published papers on application of nanofluids in various types of heat exchangers. Here, we only summarize recent investigations in this area.

Escher et al. [66] experimentally investigated laminar flow thermal performance of silica nanofluids with volume fractions up to 31% in microchannels and demonstrated that previous standard correlations can be used to estimate the convective heat transfer coefficient by using measured thermal conductivities and viscosities. Mohammadian [67] numerically simulated laminar nanofluid flow in a counterflow microchannel heat exchanger and suggested that nanofluid can enhance the heat exchanger effectiveness by Brownian motion of nanoparticles. In this study, a single-phase approach was used for nanofluid modeling and arbitrary thermal conductivity and viscosity vales were adopted in the simulation.

## **2.9 Nanofluids Experimental Setup**

The research on nanofluids has steeply accelerated with more than 2500 papers published between 2001 and 2014. The investigations on nanofluids reported in the literature can be divided into two types: (1) investigations of thermal conductivity and (29 investigations of heat transfer coefficients.

In both cases, the studies have been mainly experimental. Typically, the experimental heat transfer coefficients are compared with the heat transfer coefficients of the based fluid (i.e., the fluid in which the nanoparticles are dispersed in) and with the heat transfer coefficients calculated from well-known correlations from the literature (often called “theoretical”). The majority of measurements reported in the literature were carried out by one research group in one experimental rig.

### **Experimental Rigs**

An experimental rig can be used to measure the heat transfer coefficients of the nanofluids. A traditional setup was proposed by Haghghi [26] where a stainless-steel tube with constant heat flux on the walls was tested. Schematic diagrams of the experimental rigs used in the study are shown in Figure 5 and Figure 6. The entrance sections prior to the test sections ensured that in each rig flow was hydrodynamically fully developed and the static mixers installed at the end of the heating sections ensured uniform temperature at the outlet.

In both rigs, used in the study, the local external wall temperatures at a number of points along the test sections, the temperature at the inlet and outlet, the flow rates, and the power supply were measured, and the data were logged by a data acquisition system and set to a PC. Technical details of both rigs are summarized in Table 2. The local heat transfer coefficients were calculated from the values of the local wall and fluid temperatures and the local heat flux. From these values, the local Nusselt number were calculated. The average Nusselt numbers were calculated as the area average of the local Nusselt numbers. The heat supplied to the system was calculated from the mass flow, the specific heat, and the temperature change of the fluid.

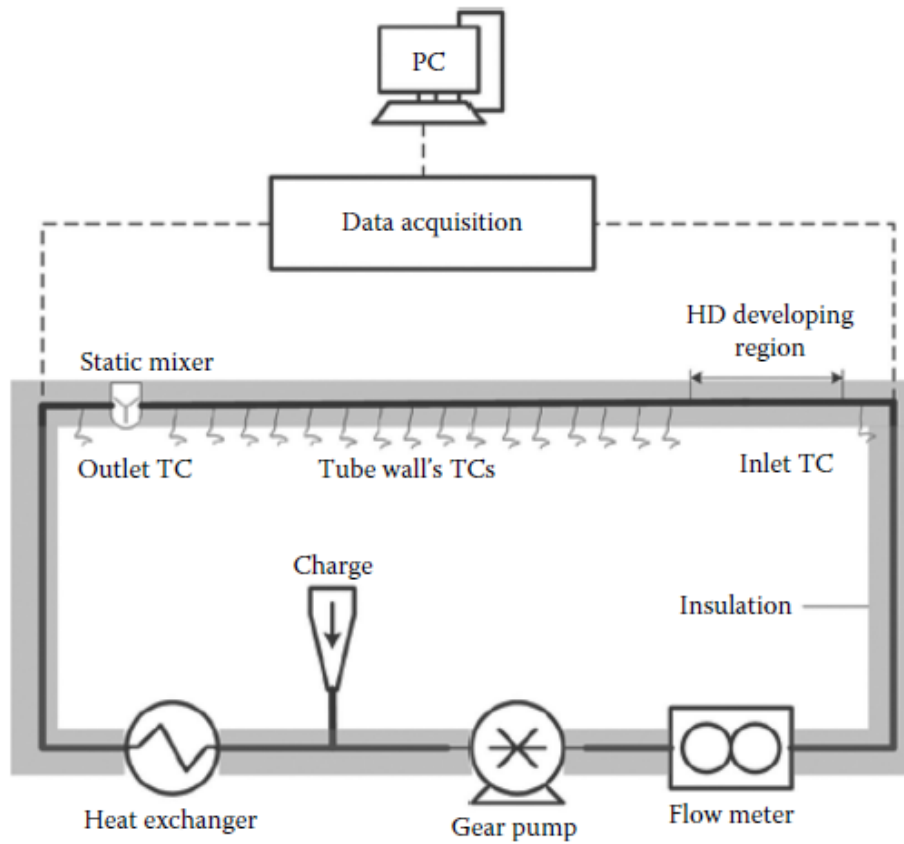


**Figure 5.** Experimental rig used by Haghighi et al. [26].

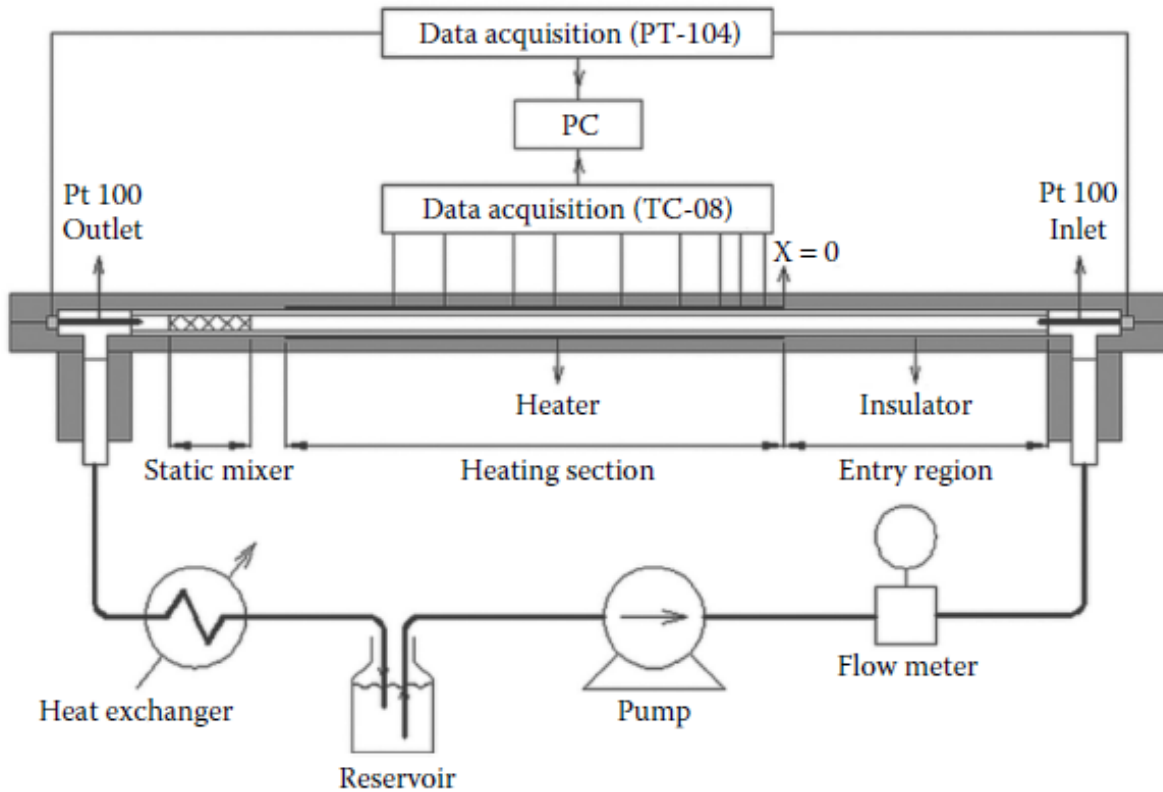


**Figure 6.** Experimental rig with TC, thermocouple; HD, hydrodynamically [26].

To assess the accuracy of the measurements in both experimental rigs, the Nusselt numbers in laminar flows of distilled water were measured in both rigs and the results were compared. As a conclusion, the heat transfer coefficients of the nanofluids measured were within similar error bands, and they were also in good agreement with the value calculated from literature correlations for laminar flows, if the correct properties of the nanofluids were used. Based on the obtained results, Haghghi et al. [26], concluded that, as far as macroscopic thermal and hydrodynamic behaviors are concerned, the nanofluids investigated behave as homogeneous mixtures and their thermal performance can be predicted from classical correlations from the literature.

**Table 3.** Details of the Test Sections [26].

Parameters	Rig 1	Rig 2
Pipe (material, $D_i$ & wall thickness)	SS, 3.70 mm, and 0.15 mm	SS, 4.57 mm, and 0.89 mm
Entrance, heating, and mixing sections	250, 1468 and 80 mm	650, 1220, and 100 mm
Temperature recording: wall, inlet, and outlet	16 T-Type (0.25 mm) thermocouples for the wall, 3 T-Type (0.5 mm) for the inlet and outlet	9 T-type (0.08 mm) thermocouples for the wall, 2Pt 100 RTD (3 mm) for the inlet and the outlet
Thermocouple positions	18, 41, 66, 110, 210, 320, 423, 528, 632, 735, 840, 945, 1050, 1160, 1260, and 1360 mm from the start of heating section	45, 105, 158, 255, 400, 562, 664, 830 and 956 mm from the start of heating section
Accuracy of temperature measurement	Better than 0.1 °c	0.03 °C at 0° for the Pt 100 RTD and 0.1°C for the thermocouples
Type of heater and power	Direct electric current through tube wall (DC), 3000 W	Electric tape heater, 300 W
Type of insulation and heat loss from the system	Armaflex foam and fiber glass insulation, less than 5%	Phenolic foam insulator, less than 5%
Pump	Gear pump (MCP-Z, Ismatec) with pump head (170.000, Micropump)	Peristaltic pump
Flow meter	Coriolis mass flow meter (CMF015 with 2700 transmitter, Micro Motion)	Coriolis mass flow meter (Optimass 3000-S3, KROHNE)
Cooling jacket	1.7 m double pipe, a plate heat exchanger, and a smaller chiller (180 W cooling capacity)	2 m double-pipe heat exchanger, chiller (400 W cooling capacity)

## 2.10 Heat Transfer Enhancement

Although an enhanced thermal conductivity in nanofluids is an encouraging feature for possible application in heat transfer devices, it is not necessarily a sufficient condition. In nanofluids should be examined for performance under convective modes.

Heat transfer is a crucial component in near all industrial process [12-16]. Consequences of improper heat transfer include non-reproducible processing conditions and lower product quality. Straight tube heat exchangers are the most common type of heat exchanger used in industrial processes due to ease of manufacturing and lower cost [12].



There are several experimental works available in the literature that study forced convective heat transfer in nanofluids as it continues to be a subject of growing importance in many applications [13-16]. A straight tube heat exchanger with laminar flow condition has a lower heat transfer coefficient (HTC) as compared to turbulent flow conditions. The heat transfer performance can be enhanced either by geometry perturbation or by the improvement of the fluid properties.

It has been shown that the thermal properties of a nanofluid appear to be higher than those of the base fluid. Hence, nanofluids appear to be an interesting alternative for advanced thermal applications for microscale and nanoscale heat transfer. Alumina oxide nanoparticles ( $\text{Al}_2\text{O}_3$ ) has been widely used for both experimental and numerical work [17-26].

Wen and Ding [17] developed a series of experiments using  $\text{Al}_2\text{O}_3$ -water nanofluids in a circular tube. It was observed that the local HTC enhanced by 47%, using  $\text{Al}_2\text{O}_3$  nanoparticles for  $\phi_b = 1.6\%$ , in the laminar flow regime. Maïga et al. [18] investigated  $\text{Al}_2\text{O}_3$ -water and  $\text{Al}_2\text{O}_3$ -ethylene glycol under constant heat flux boundary condition. The reported results show a 63% enhancement in HTC for 7.5% particle loading. Heris et al. [19] studied the laminar convective heat transfer of  $\text{CuO}$ -water and  $\text{Al}_2\text{O}_3$ -water nanofluids flow in the straight tube and reported that the HTC increases with an increase in particle loading and a decrease in the particle size. The HTC was augmented by 40% for  $\text{Al}_2\text{O}_3$ -water at  $\phi_b = 2.5\%$ . Anoop et al. [20] conducted experiments using an aqueous solution of  $\text{Al}_2\text{O}_3$ -water in the developing region of a pipe flow to calculate the HTC considering the influence of particle size. The experimental results showed a 25% HTC enhancement for a 45 nm particle size and 11% for a 150 nm particle size. It was concluded that heat transfer enhancement was not only due to the intensification in thermal conductivity but also because of the effects of particle migration and thermal dispersion. Hwang et al. [21] measured the pressure drop and convective heat transfer of water-based  $\text{Al}_2\text{O}_3$  nanofluids flowing through a uniformly heated circular tube in the fully developed laminar flow regime. The experimental results showed that the HTC increases up to 8%, at  $\phi_b = 0.3\%$  as compared to water.

Davarnejad et al. [22] performed simulations to investigate the heat transfer characteristics of water-based  $\text{Al}_2\text{O}_3$  nanofluid with  $\phi_b = 0.5\% - 2.5\%$ , in a circular tube under constant heat flux and laminar flow conditions. It was reported that HTC enhanced marginally by 6% at  $\phi_b = 2.5\%$ , as compared to the water. Kim et al. [23] investigated the effect of nanofluids on convective heat transfer through a circular straight tube with constant heat flux condition under both the laminar and turbulent flow regimes.

For  $\text{Al}_2\text{O}_3$  nanofluids with  $\phi_b = 3\%$ , the thermal conductivity and HTC increases by 8% and 20%, respectively. The enhancement of the convective HTC at the entrance region was due to the Brownian motion of the nanoparticles. Rea et al. [24] investigated the laminar convective heat transfer and viscous pressure loss for  $\text{Al}_2\text{O}_3$ -water and  $\text{ZrO}_2$ -water nanofluids flow in a vertical heated tube. The HTC's in the entrance and fully developed regions were found to be enhanced by 17% and 27%, respectively, for water-based  $\text{Al}_2\text{O}_3$  nanofluid at  $\phi_b = 6\%$ , as compared to the water. Purohit et al. [25] studied the laminar forced convective heat transfer in a circular tube for three different nanofluids ( $\text{Al}_2\text{O}_3$ -water,  $\text{ZrO}_2$ -water and  $\text{TiO}_2$ -water). They reported that for the same Re comparison criteria, the HTC for nanofluids is found to be significantly higher (18%) as compared to the base fluid. Haghghi et al. [26] investigated the heat transfer characteristics of a straight microtube for three different nanofluids ( $\text{Al}_2\text{O}_3$ -water,  $\text{ZrO}_2$ -water and  $\text{TiO}_2$ -water) under laminar condition ( $\text{Re} = 200 - 2200$ ). For the nanofluids considered, the HTC was reported enhanced by 23% as compared to water.

The extensive studies, both experimental and theoretical have been conducted to calculate the convective HTC of the nanofluids flow in straight tube. It is conclusive from the literature review that the HTC not only enhanced by the thermal conductivity but also due to the disturbances of thermal boundary layer caused by the Brownian motion of the nanoparticles. It may also be noted that there are only few studies with a wider range of nanoparticles and particle concentrations. This is mainly because the experimental analysis can be complicated for the wider range of the design parameters.

## Enhancement Mechanisms

Many explanations have been given by different research groups for the enhancement of convective heat transfer in Nanofluids. Mechanisms proposed to explain the enhancement include Brownian motion of nanoparticles, liquid layering of the base fluid surrounding nanoparticles, and nanoparticle aggregation. However, which, if any, of these possible mechanisms is mainly responsible for the thermal enhancement is still under debate.

- **Brownian Motion:** Nanoparticles move through the molecules of the base fluid and sometimes collide with each other by means of Brownian motion. Particularly, when two particles collide, the solid-solid heat transfer mode could increase the overall thermal conductivity of the nanofluid. The effect of Brownian motion is a diffusive process with a diffusion constant  $D$  given by the stokes-Einstein formula:  $D = k_B T / 3 \pi \eta d$ . The higher the temperature, the higher the diffusivity, and thus the higher the thermal conductivity.
- **Liquid layering:** A liquid in contact with a solid interface is more ordered than the bulk liquid. The interaction between the atoms of the liquid and the solid generates an oscillatory behaviour in the liquid density profile in the direction normal to the interface. The strength of the solid-liquid bonding determines the magnitude of the layer, which can even extend up to several molecular distances for sufficiently strong interactions. These structural changes in the liquid structure have shown to have significant effects on various properties.
- **Nanoparticle aggregation:** Nanoparticles have been experimentally observed to agglomerate into clusters when suspended in the liquid. In theory, nanoparticle clustering into percolating patterns creates paths of lower thermal resistance that would have a major effect on the overall thermal conductivity and viscosity. The effect on thermal conductivity enhancement would, however, be negated for low particle volume fractions, because there would be particle-free areas in the liquid.

## 2.11 Modeling Convection in Nanofluids

An important study of convective transport in nanofluids was made by Buongiorno [39]. He focused on the heat transfer enhancement observed in convective solutions. Buongiorno concluded that turbulence is not affected by the presence of the nanoparticles so this cannot explain the observed enhancement. Particle rotation has also been proposed as a cause of heat transfer enhancement, but Buongiorno calculated that this effect is too small to explain the observed results. With dispersion, turbulence, and particle rotation ruled out as significant agencies for heat transfer enhancement, Buongiorno proposed a new model based the mechanics of the nanoparticle/base fluid relative velocity.

This researcher noted that the nanoparticle absolute velocity can be viewed as the sum of the based fluid velocity and a relative velocity (normally called the slip velocity). He then considered seven slip mechanisms: inertia, Brownian diffusion, thermophoresis, diffusiophoresis, Magnus effect, fluid drainage, and gravity settling. He concluded that in the absence of turbulent effects, it is the Brownian diffusion and the thermophoresis that will be important.

He proceeded to write down conservation equations based on these two effects. The Buongiorno model treats the nanofluid as a two-component mixture (base fluid and nanoparticles) with the following assumptions:

1. Incompressible flow
2. No chemical reactions
3. Negligible external forces
4. Dilute mixture
5. Negligible viscous dissipation
6. Negligible radiation heat transfer
7. Nanoparticles and based fluid locally in thermal equilibrium

The continuity equation for the nanofluid is:

$$\nabla \cdot v = 0 \quad (24)$$

where  $v$  is the nanofluid velocity.

The conservation equation for the nanoparticles in the absence of chemical reactions is:

$$\frac{\partial \phi}{\partial t} + v \cdot \nabla \phi = -\frac{1}{\rho_p} \nabla \cdot j_p \quad (25)$$

where:

$t$  is the TIME

$\phi$  is the nanoparticle volume fraction

$\rho_p$  is the nanoparticle mass density

$j_p$  is the diffusion mass flux for the nanoparticles, given as the sum of two diffusion terms (Brownian diffusion and thermophoresis)

Thermophoresis is analogous to the Soret effect in gaseous or liquid mixtures. It should be noted that Buongiorno departed from the usual tradition by using the notation in which the dependence on temperature of the thermophoretic coefficient is considered explicitly. Thus,  $D_T$  has the same dimensions as  $D_B$ . Here,  $D_B$  is the Brownian diffusion coefficient given by the Einstein- Stokes equation:

$$D_B = \frac{k_B T}{3\pi\mu d_p} \quad (26)$$

where:

$k_B$  is the Boltzmann constant

$\mu$  is the viscosity of the fluid

$d_p$  is the nanoparticle diameter

Equation 24 and 25 then produce an equation expressing the conservation of nanoparticles in the form:

$$\frac{\partial \phi}{\partial t} + v \cdot \nabla \phi = \nabla \cdot \left( D_B \nabla \phi + D_T \frac{\nabla T}{T} \right) \quad (27)$$

The momentum equation for a nanofluid takes the same form as for a pure fluid, but it should be remembered that  $\mu$  is a strong function of  $\phi$ .

If one introduces a buoyancy force and adopts the Boussinesq approximation, then the momentum equation can be written as:

$$\rho \left( \frac{\partial v}{\partial t} + v \cdot \nabla v \right) = -\nabla_p + \mu \nabla^2 v + \rho g \quad (28)$$

The thermal energy equation for a nanofluid can be written as:

$$\rho c \left( \frac{\partial T}{\partial t} + v \cdot \nabla T \right) = -\nabla \cdot q + h_p \nabla \cdot j_p \quad (29)$$

where:

$c$  is the nanofluid specific heat

$T$  is the nanofluid temperature

$h_p$  is the specific enthalpy of the nanoparticle material

$q$  is the energy flux, relative to a frame moving with the nanofluid velocity  $v$

### **Nanofluid Stability**

Nanoparticles are often hydrophobic and therefore cannot typically be dispersed in most heat transfer fluids such as water or ethylene glycol without surface treatments and/or dispersants or surfactants. Furthermore, without these special treatments, the nanoparticles would most certainly agglomerate and/or settle, thereby creating other problems such as channel clogging and a reduction in thermal conductivity of the mixture. Surfactants or dispersion agents are therefore commonly used in nanofluids.

Although they are beneficial for stabilizing the suspension, they may also create certain problems for heat transfer mediums. Wang [29] considered the dispersion behaviour of aqueous copper nano-suspensions for various pH value and different dispersant types and concentrations. Dispersant agents (or surfactants) included hexadecyl trimethyl ammonium bromide, sodium dodecylbenzenesulfonate (SDBS), and polyoxy-ethylene nonylphenyl ether (TX-10). Results clearly show that surfactants lead to the enhancement of the stability of Cu suspensions.

Stability of mixtures remains an issue for which more investigation is required. Long-term stability, and the stability after thousands of thermal cycles are questions that will need to be addressed more carefully so in this study the effect of the surfactants was not included.

## Chapter

### 3 Mathematical Formulation

The mathematical modeling of the nanofluids is done using single phase approach. Single-phase models (SPH) including dispersion model (SPD) assumes that the base fluid and the nanoparticles have the same temperature and velocity field. Therefore, the single phase nanofluid flow was assumed as a steady incompressible flow and the continuity, momentum and energy equations are solved using the effective properties of the nanofluids. Similar assumptions were made in the literature for the single phase nanofluid flow [27-28].

#### 3.1 Governing Equations

The present study was conducted for both the constant heat flux ( $q_w'' = 10,000 \text{ W/m}^2$ ) and constant wall temperature ( $T_w = 313.15 \text{ K}$ ) boundary conditions. At the inlet, the uniform axial velocity  $u_o$  and initial temperature ( $T_o = 293 \text{ K}$ ) were assumed.

The fully developed conditions are assumed at the tube exit section, which means all axial derivatives are zero. No-slip condition and uniform heat flux are imposed on the tube wall. The continuity, momentum and energy equations subject to above boundary conditions were solved using finite volume approach/method. The governing equations are expressed as follows:

$$\nabla \cdot (\rho_{eff} \vec{V}) = 0 \quad (30)$$

$$\rho_{eff} (\vec{V} \cdot \nabla \vec{V}) = -\nabla P + \nabla \cdot (\mu_{eff} \nabla \vec{V}) \quad (31)$$

$$\nabla \cdot (\rho_{eff} c_{eff} \vec{V} T) = \nabla \cdot (k_{eff} \nabla T) \quad (32)$$

where  $\rho_{eff}$ ,  $\mu_{eff}$ ,  $C_{eff}$ ,  $k_{eff}$  are the density, effective viscosity, specific heat and effective thermal conductivity of the nanofluid, respectively.

### 3.2 Geometrical Configuration

In the present study, different geometrical scales (conventional straight tube and conventional straight microtube) are considered for investigating laminar nanofluids flow as shown in Figure 7. The ratio of  $L/D$  is so chosen to maintain a hydro-dynamically developed flow at the outlet. The circular straight tube has a diameter of 10 mm and a length of 5.34 meters. The straight microtube has a diameter of 0.5 mm and a length of 0.3 meters. This geometry was selected as it is commonly used in industrial applications.

The computational domains are considered to be three-dimensional for better comparison of the nanofluid flow inside the geometries. It can be discussed that 2D axisymmetric is only able to capture radial migration of nanoparticles inside the fluid, while the difference between 3D model and 2D axisymmetric simulation results prove that nanoparticles migrate from the wall both radially and tangentially.

The details of the geometries used to carry out the numerical simulations laminar nanofluids flow are shown in Table 3.

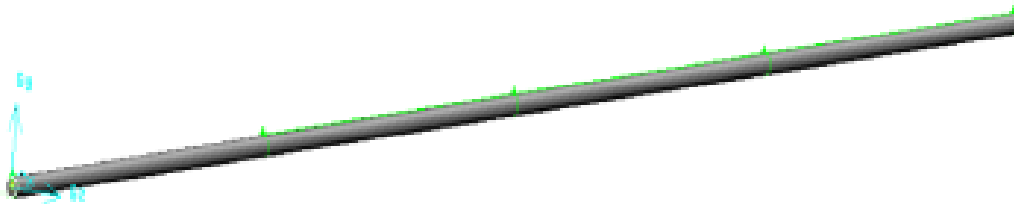


**Figure 7.** Computational domain: straight tube and straight microtube.

**Table 4.** Details of the geometries considered for the numerical study.

Geometry (scale)	$d_i$ (mm)	L (m)
Straight tube	10	5.34
Straight Microtube	0.5	0.3



Through this investigation, it might be noted that the geometry (scale) has an important effect in the heat transfer performance of the nanofluids. Hydrodynamics play a critical role in determining the thermal performance of any heat transfer device. For example, Singh et al. [43] reported that the helical coil tube provides a higher heat transfer performance as compared to straight tube. In the study, in a helical coil, the Nusselt number got enhanced approximately by 2.5 times compared to straight tube for 4% nanoparticle volume fraction. The enhancement in heat transfer is attributed to the change in physics of fluid flow due to geometry perturbation.

In the helically coiled tubes, there is a modification of the flow due to the Dean roll cells, which produce a secondary flow field with a circulatory motion, pushing the fluid particles toward the core region of the tube.

The laminar flow persists at a much higher Reynolds number in helical coils as compared to straight tube because of the stabilizing effects of the secondary flow. Consequently, the differences in heat transfer performance between coils and straight tubes are particularly distinct in the laminar flow region. However, the Dean roll cells divide the cross-section into two zones in which the isotherms forms closed curves. Fluid particles inside the Dean roll cells are prevented from approaching the hot walls; thus, mixing is poor, giving rise to a heterogenous temperature field.

### **3.2 Thermophysical Properties**

In SPH, the properties of the fluids are assumed constant. The dissipation and pressure work are neglected. It was also assumed that the fluid phase and nanoparticles are in thermal equilibrium with zero relative velocity. The effective density ( $\rho_{eff}$ ) and specific heat ( $C_{p,eff}$ ) of the nanofluids were calculated based on the mixture rule explained by Wang et al. [29]. To examine the validity of  $\rho_{eff}$  and  $C_{p,eff}$  equations, other similar studies by Pak et al. [30], Ho et al. [31], Das et al. [32] and Khanafer et al. [33] were reviewed.

For viscosity, different models can be found in the literature for the effective viscosity of nanofluids as a function of volume fraction. Brinkman et al. [34] presented a viscosity correlation for concentrated suspensions of nanoparticles.

Lundgren et al. [35] proposed the viscosity model in form of the Taylor series. Batchelor et al. [36] studied the effect of Brownian motion of the rigid spherical particles on the effective viscosity. For the effective thermal conductivity, Hamilton et al. [37] presented a definition of a two-components mixture. Maxwell [38] proposed a model for solid-liquid mixture with relatively large particles. Buongiorno et al. [39] justified the use of the Maxwell model for calculating the thermal conductivity of water-based nanofluids.

Table 4 shows the summary of the equations reviewed during this study. For computational purposes the equations from Wang et al. [29], Khanafer et al. [33], Batchelor et al. [36] and Purohit et al. [25] were used to calculate the thermophysical properties of the nanofluids.

**Table 5.** Thermophysical properties equations of nanoparticles.

Properties	Author	Equations
Density (kg/m <sup>3</sup> )	Wang et al. [29]	$\rho_{eff} = \left(\frac{m}{V}\right)_{eff} = \frac{m_b+m_p}{V_b+V_p} = \frac{\rho_b V_b + \rho_p V_p}{V_b+V_p} = (1 - \phi_b)\rho_b + \phi_b\rho_p$ $\phi_b = \frac{V_p}{V_f+V_p}$ is the volume fraction of the nanoparticles
Specific Heat (J/kg-K)	Das et al. [32] Khanafer et al. [33]	$c_{eff} = (1 - \phi_b)c_f + \phi_b c_p$ $c_{eff} = \frac{(1-\phi_b)\rho_f c_f + \phi_b \rho_p c_p}{\rho_{eff}}$
Viscosity (kg/m-s)	Brinkman [34] Lundgren [35] Batchelor et al. [36]	$\mu_{eff} = 1/(1 - \phi_b)^{2.5} = (1 + 2.5\phi_b + 4.375\phi_b^2 + \dots)\mu_f$ $\mu_{eff} = \frac{1}{1-2.5\phi_b} \mu_f = (1 + 2.5\phi_b + 6.25\phi_b^2 + O(\phi_b^3)) \mu_f$ $\mu_{eff} = (1 + 2.5\phi_b + 6.2\phi_b^2)\mu_f$
Thermal Conductivity (W/m-K)	Maxwell et al. [37] Hamilton et al. [38] Purohit et al. [25]	$k_{eff} = \frac{k_p+2k_f+2\phi_b(k_p-k_f)}{k_p+2k_f-\phi_b(k_p-k_f)} k_f = k_f + \frac{3\phi_b(k_p-k_f)}{k_p+2k_f-\phi_b(k_p-k_f)}$ $k_{eff} = \frac{k_f(1-\phi_p)\left(\frac{dT}{dx}\right)_f + k_p\phi_p\left(\frac{dT}{dx}\right)_p}{\phi_p\left(\frac{dT}{dx}\right)_p + (1-\phi_p)\left(\frac{dT}{dx}\right)_f}$ $k_{eff} = \frac{k_p + 2k_f + 2\left(\frac{k_p}{k_f}\right)\phi_b}{k_p + 2k_f - (k_p - k_f)\phi_b}$

The thermophysical properties equations to evaluate the SPD model were expressed as [27]:

$$k_{eff} = k_{nf} + k_{disp} \quad (33)$$

$$k_{disp} = C(\rho C_p)_{nf} uR \quad (34)$$

$$\mu_{eff} = \mu_{nf} + \mu_{disp} \quad (35)$$

$$\mu_{disp} = \frac{k_{disp}}{C_{p,bf}} Pr_{nf} \quad (36)$$

where,  $k_{disp}$  is the dispersion thermal conductivity,  $C$  is an experimental data constant from Wen et al. [17],  $u$  is the mean velocity,  $R$  is the inner radius and  $\mu_{disp}$  is the dispersion viscosity.

The thermophysical properties of the base fluids (water, ethylene glycol and oil) and nanoparticles ( $Al_2O_3$ ,  $CuO$ ,  $TiO_2$ ,  $SiO_2$ ,  $ZnO$ ) are specified in Table 5 and Table 6, respectively. These properties were adopted from Sarkar [40], Tertsinidou et al. [41] and Heris et al. [42]. In this study, the nanofluids effective properties has an important effect on the obtained results. There has been a large number of theories and correlations that have been used and developed for these thermophysical properties with predictions and conclusions that can be different. The thermophysical properties of nanofluids are influenced by the concentration of nanoparticles. The density, viscosity and thermal conductivity of nanofluids increases with increase in nanoparticle concentration. The specific heat capacity decreases with increase in the volume fraction.

**Table 6.** Thermophysical properties of different base liquid types.

Base liquid type	Density ( $kg/m^3$ )	Specific Heat ( $J/kg-K$ )	Viscosity ( $kg/m-s$ )	Thermal Conductivity ( $W/m-K$ )	Pr
Water	997	4170	$1.00 (10)^{-3}$	0.606	6.96
Ethylene-Glycol	1111	2415	$1.57 (10)^{-2}$	0.252	150.46
Oil (Turbine)	868	2000	$2.70 (10)^{-2}$	0.120	462.55

**Table 7.** Thermophysical properties of different nanoparticles types.

Nanoparticle type	Density (kg/m <sup>3</sup> )	Specific Heat (J/kg-K)	Thermal Conductivity (W/m-K)
Al <sub>2</sub> O <sub>3</sub>	3970	791	40.00
TiO <sub>2</sub>	3900	692	8.40
CuO	6400	551	32.90
SiO <sub>2</sub>	2200	745	1.40
ZnO	5600	495	13.00

### 3.3 Grid Independence Test

The governing equations of mass, momentum and energy were solved using finite volume approach/method. The semi implicit method for pressure linked equations (SIMPLE) was employed to couple pressure and velocity in equations.

A second order upwind scheme was employed for interpolating the parameters. The structured grid distribution was used to discretize the computational domain. To ensure the accuracy and the consistency of computational results, various uniform grids were tested as shown in Table 7. The selected grid for the study calculations consisted of 532 and 30 nodes in the axial and radial directions, respectively. The numerical computations were considered converged, when the residual summed over all the computational nodes at  $i^{\text{th}}$  iteration,  $R_j^i$ , satisfies the following criterion:  $(R_j^i/R_j^m) \leq 10^{-6}$ , where  $R_j^m$  denotes the maximum residual value of  $j$  variable after  $m$  iterations, and  $j$  is applied for pressure, velocity and temperature.

**Table 8.** Mesh Independency Test.

Grid Size	Nusselt Number	Computational time (s) (Single-phase)	Computational time (s) (Two-phase)
534 x 10	5.80	70	550
534 x 20	5.85	75	570
534 x 30	5.94	77	580
534 x 40	5.94	81	600

Computational time was the second parameter considered during the numerical simulation of nanofluids convective heat transfer. The major drawback of two-phase models is their computational expense. The required CPU time was measured as 600 s for using a two-phase model compared with 81 s for using the single-phase model for Al<sub>2</sub>O<sub>3</sub>-water nanofluid flow at a Reynolds number of 500. The numerical studies presented in this study were performed on a workstation operating with an Intel Core 2.5 GHz CPU used only for calculations.

The local and average HTC's were calculated using equation (37) & (38), respectively.

$$h_x = \frac{q''}{T_w(x) - T_m(x)} \quad (37)$$

$$h_{avg} = \frac{1}{L} \int_0^L h(x) dx \quad (38)$$

The Nusselt number (Nu), was defined as:

$$Nu(x) = \frac{(h_x D)}{k} \quad (39)$$

The wall and fluid temperatures and the heat flux were computed to calculate the convective HTC. For constant heat flux, the fluid mean temperature ( $T_m$ ) was computed as follows:

$$T_m = \frac{1}{v_{avg} A} \int_0^A u T dA \quad (40)$$

The effectiveness of the single and two-phase models in terms of their computational expense

## Chapter

### 4 Results and Discussion

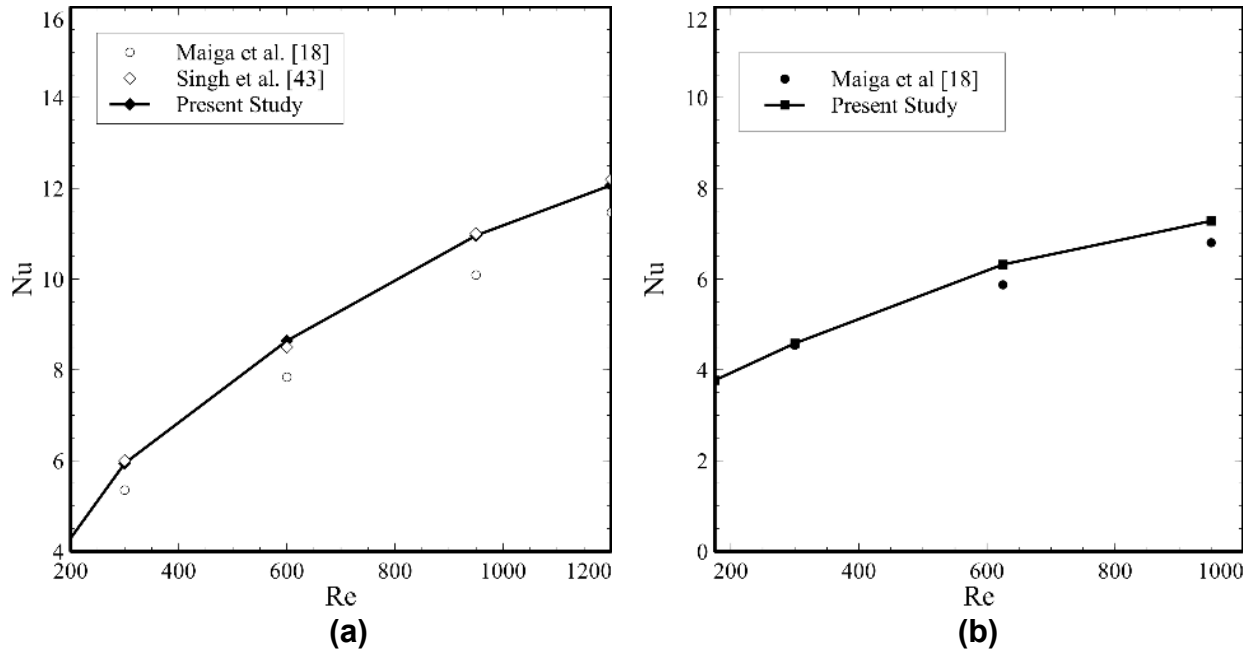
An extensive number of numerical simulations ( $> 500$ ) were performed to determine the HTC enhancement of laminar nanofluids. For validation purpose, the present results of the Nusselt number for straight tube were compared with the correlation ( $Nu = 0.086Re^{0.55}Pr^{0.5}$ ) of Maïga et al. [18] and the computational results of Singh et al. [43] for constant heat flux condition.

Figure 8a shows a good agreement of the present results with the literature [18, 43] for water-based  $Al_2O_3$  nanofluid at  $\phi_b = 1\%$ . The Nu results were also validated for constant wall temperature condition as shown in Figure 8b. It may be noted that there is a good agreement between the present results and results predicted by Maïga et al. [18] ( $Nu = 0.28Re^{0.35}Pr^{0.36}$ ), for the  $Al_2O_3$ -water based nanofluid with  $\phi_b = 4\%$ . In this study, six different cases with different combinations of the geometry (scale), nanoparticles concentration and base fluids were considered as shown in Table 8.

It may be noted from Table 7, that three different base fluids and five different nanofluids with wide range of particle volume fractions ( $0 \leq \phi_b \leq 10\%$ ) are considered for the detailed investigation.

**Table 9.** Cases considered to determine the HTC enhancement of nanofluids.

Case	Base Fluid	Nanoparticles	B. Condition	Model	%vol	Geometry (scale)
1	Water	$Al_2O_3$ , $TiO_2$ , $CuO$ , $SiO_2$ , $ZnO$	Cst. Heat Flux	SPH	0–10	S. Tube
2	EG	Same as prev.	Cst. Heat Flux	SPH	0–10	S. Tube
3	Oil	Same as prev.	Cst. Heat Flux	SPH	0–10	S. Tube
4	Water	Same as prev.	Cst. Temp.	SPH	0–10	S. Tube
5	Water	Same as prev.	Cst. Heat Flux	SPH	0–10	Microtube
6	Water	Same as prev.	Cst. Heat Flux	SPD	0–10	S. Tube



**Figure 8.** Comparison of Nu for Al<sub>2</sub>O<sub>3</sub>-water nanofluid (a) constant heat flux condition at  $\phi_b = 1\%$ . (b) constant wall temperature condition at  $\phi_b = 4\%$ .

#### 4.1 Case 1: Water nanofluid in st. tube with constant heat flux using SPH

In the first case water-based nanofluids with the constant wall heat flux ( $q_w'' = 10,000$  W/m<sup>2</sup>) were considered. Figure 9 shows the results for the fluid temperature in the radial direction and the wall temperature at the constant values of Re = 500 and T<sub>o</sub> = 293.15 K. It may be noted from Figure 9a, that the fluid temperature decreases with an increase of the nanoparticle concentration from 0 to 10%, especially near the tube wall, suggesting a higher heat transfer rate (above 10%) with nanoparticles.

Figure 9b demonstrates the diminution of the wall temperature at different nanoparticle concentrations. The wall temperature decreases by 40 K for the Al<sub>2</sub>O<sub>3</sub>-water nanofluid with nanoparticle concentrations from 0 to 10%. The diminution in temperature reflects a better heat transfer rate at the tube wall. These effects may be explained by the fact that with the presence of the nanoparticles, the thermal properties of the resulting mixture have become more important as the product of  $\rho C_p$  and the thermal conductivity have increase with respect to pure water.

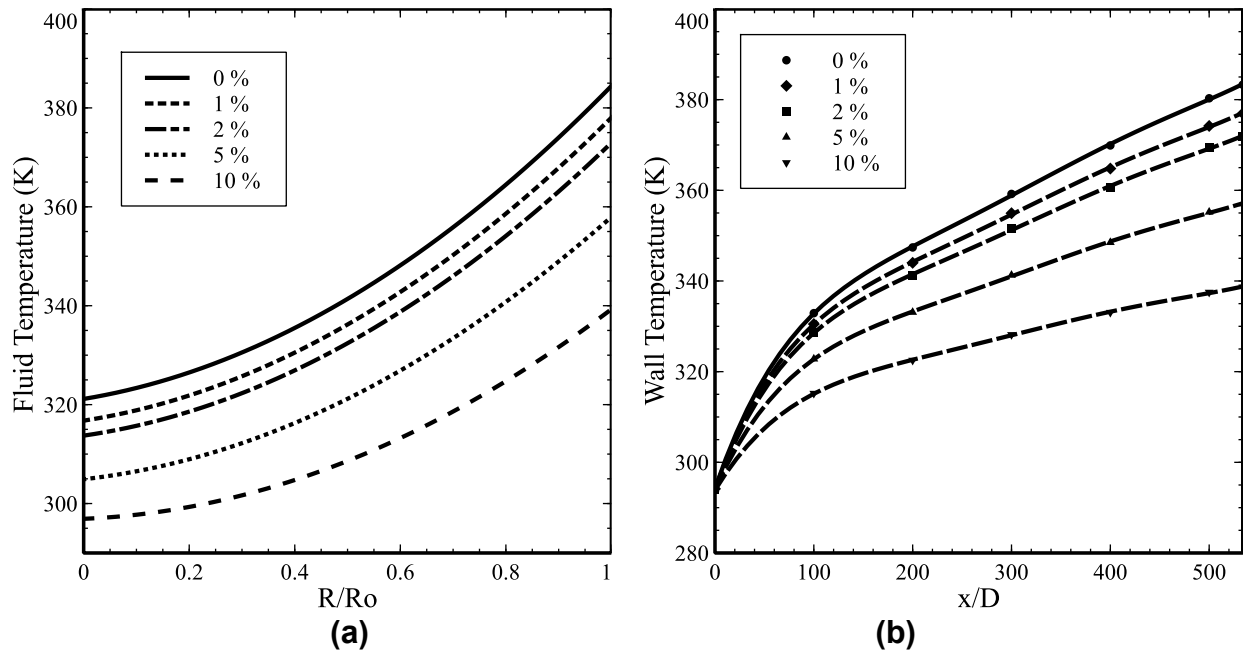
Figure 10 shows the effect of nanoparticle concentration on the fluid mean temperature and wall temperature in axial direction. It may be noted from Figure 10a, that the fluid mean temperature decreases with an increase in the value of  $\phi_b$ . The decrease in the fluid mean temperature is caused mainly due to the higher thermal conductivity (up to 32%) of the  $\text{Al}_2\text{O}_3$ -water nanofluid. The radial, wall and fluid mean temperatures demonstrate that  $\text{Al}_2\text{O}_3$ -water nanofluid offers a higher thermal capacity as compared to the water. It may also be observed that at the higher thermal conductivity, the wall-to-fluid heat transfer is more important as it augments the heat transfer rate. Three nanoparticles ( $\text{Al}_2\text{O}_3$ ,  $\text{TiO}_2$  and  $\text{CuO}$ ) with two different concentrations ( $\phi_b = 1\%$  and  $\phi_b = 10\%$ ) were considered to investigate the thermal efficiency of the nanofluids with increase in the particle concentrations as shown in Figure 10b.

For the higher nanoparticle concentration ( $\phi_b = 10\%$ ), the wall temperature for  $\text{Al}_2\text{O}_3$ -water nanofluid is lower than the  $\text{TiO}_2$ -water and  $\text{CuO}$ -water nanofluids. This lower temperature can be mainly explained with the higher values of thermal conductivity which is 4% higher as compared to  $\text{TiO}_2$ -water and 1% higher as compared to  $\text{CuO}$ -water. The results revealed that  $\text{Al}_2\text{O}_3$ -water nanofluids will have a higher transfer coefficient (at least 1%) than the other two nanofluids considered.

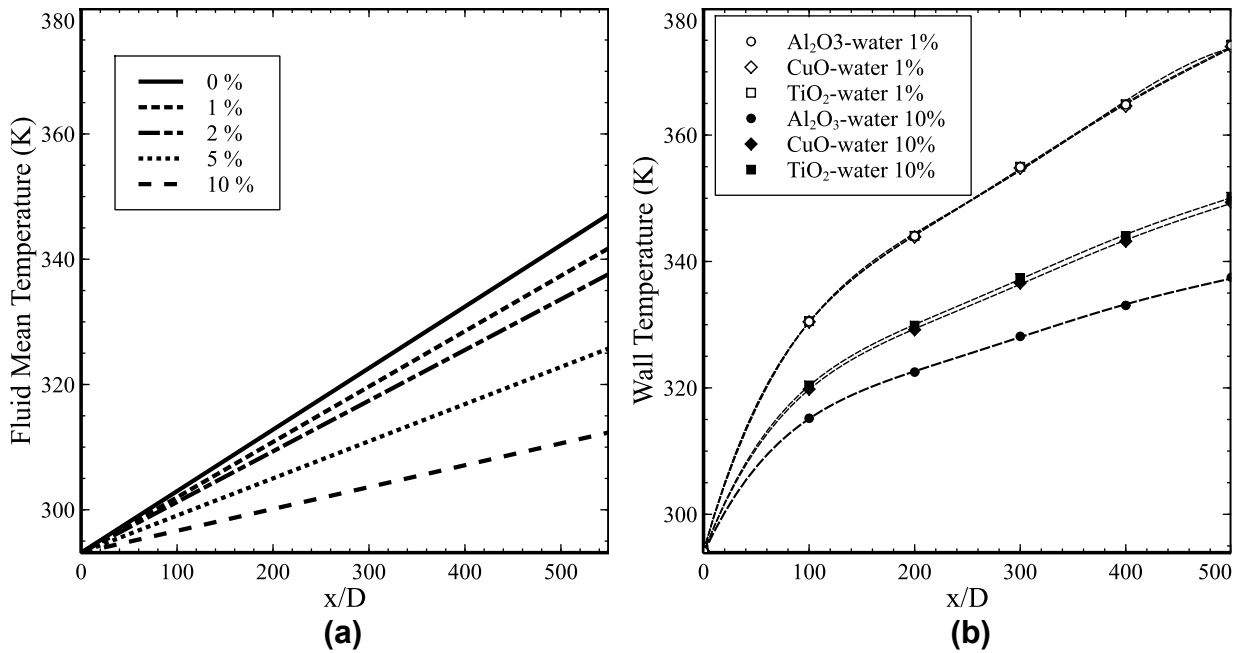
The nanoparticles concentration has significant effect on heat transfer performance. A larger number of nanoparticles in the base-fluid increases the thermal conductivity of the nanofluid but it is accompanied with higher values of the wall shear stress.

Although, the use of nanofluids has heat transfer enhancement capabilities due to their increase viscosity, they will also increase friction/pressure losses. For example, Maïga et al. [18] found that there is a 2.5-fold increase in the wall shear stress with a  $\phi_b = 5\%$  for an  $\text{Al}_2\text{O}_3$ -water nanofluid. Because this friction/pressure losses, the benefits of the higher transfer rates versus the corresponding and drastic increases in viscosity have to be considered. In this study, two different nanoparticle concentrations ( $\phi_b = 1\%$  and  $\phi_b = 4\%$ ) of the water-based  $\text{Al}_2\text{O}_3$  nanofluid were used to determine the effect of the nanoparticle concentration.





**Figure 9.** Effect of nanoparticle concentration in tube flow: (a) fluid temperature profiles at tube exit, (b) axial development of wall temperature.



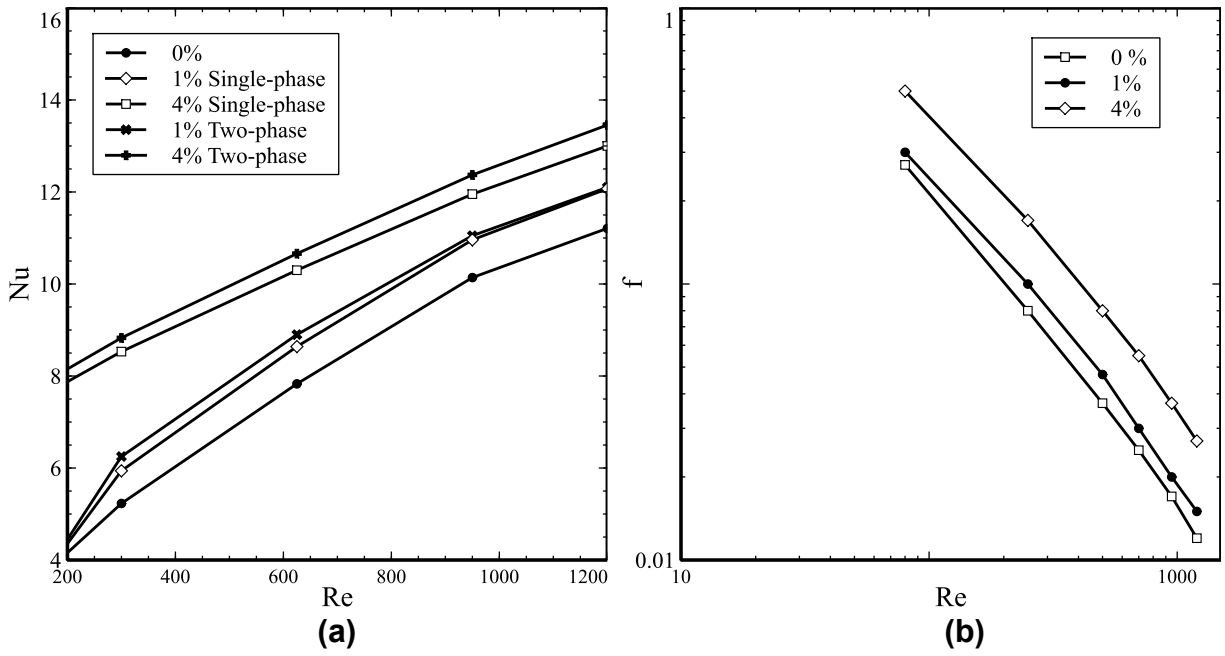
**Figure 10.** Effect of nanoparticle concentration in tube flow: (a) axial development of  $T_m$ , (b) axial development of wall temperatures.

Figure 11a shows that the Nu increases with an increase in nanoparticle concentration for any given value of Re. This is mainly because the nanoparticles increase the thermal conductivity of the base fluid and, hence, augments the convective heat transfer. At low Re (below 100) the Nu is 2.2 times higher for  $\phi_b = 4\%$  as compared to  $\phi_b = 1\%$ . For high Re (above 1000) Nu increases less than 10%. Additionally, in Figure 11, the single-phase and two-phase models were compared. It can be said that the two-phase model present higher values of Nusselt numbers, however their results are quite similar (maximum difference of 5%). As stated by Bianco [48], this is a good result, as the single-phase model requires information about just particles and base fluid.

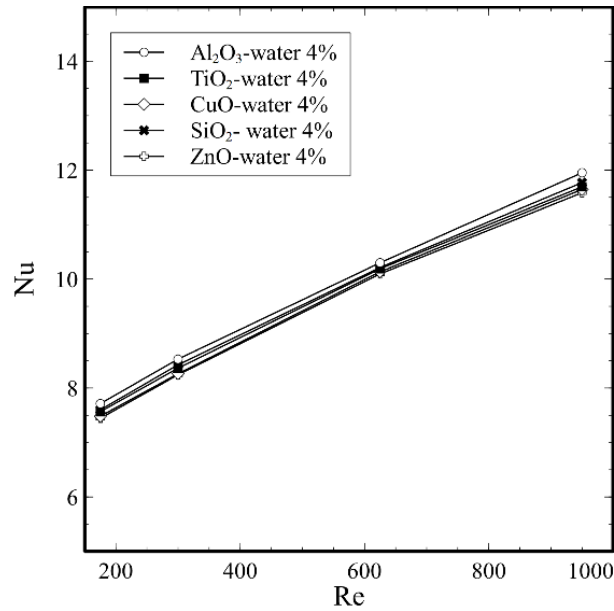
Figure 11b shows the effect of particle volume fraction and Reynolds number on friction factor in straight tube. The friction factor increases by 13% and 38% with 1% and 4% increase in the nanoparticle concentration, respectively, for a given value of Re. The larger the value of viscosity, the more growth in axial pressure drop. The Brownian motion, dispersion, and fluctuation of nanoparticles, especially near the wall of tubes, leads to an intensifying of the momentum exchange rates between particles. This momentum exchange can considerably increase axial pressure drop. Considering this reduction of Nu and the increases of the wall shear stresses using more than  $\phi_b = 5\%$ , a higher nanoparticle concentration would have to be determined by the specific application.

Figure 12 shows a comparison of Nu for the different nanoparticles considered. Among the nanoparticles studied  $\text{Al}_2\text{O}_3$ ,  $\text{TiO}_2$ ,  $\text{CuO}$ ,  $\text{SiO}_2$ ,  $\text{ZnO}$  there is evidence that the  $\text{Al}_2\text{O}_3$  nanofluid has a marginally higher value (by 4%) of Nu for the  $\text{Al}_2\text{O}_3$ -water based nanofluid as compared to the  $\text{ZnO}$ -water nanofluid.

This enhancement in the Nu is relatively lower as the Pr of all the selected nanofluids are in the range of 6.7 to 7.3 at  $\phi_b = 4\%$ . The Nu of  $\text{SiO}_2$ -water nanofluid was the second highest since  $\text{SiO}_2$  nanofluid has the highest average velocity among the fluids because of the lowest value of density ( $\rho = 1046 \text{ kg/m}^3$ ). The result indicate that the fluid velocity plays a role on the heat transfer.



**Figure 11.** Comparison for an Al<sub>2</sub>O<sub>3</sub>-water nanofluid at  $\phi_b = 0\%$ , 1% and 4%: (a) Nusselt Number (b) Friction Factor



**Figure 12.** Comparison of Nu for water-based nanofluids at  $\phi_b = 4\%$ .

## 4.2 Case 2: Ethylene glycol nanofluid in st. tube with constant heat flux using SPH

This case considers ethylene-glycol (EG) base nanofluids with equal parameters as previous case for comparison purposes. Figure 13 shows the axial development of the wall temperatures at lower ( $\phi_b = 1\%$ ) and higher ( $\phi_b = 10\%$ ) values of nanoparticle concentration. For lower nanoparticle concentration ( $\phi_b = 1\%$ ), the  $T_w$  with  $\text{Al}_2\text{O}_3$ -EG nanofluid is approximately the same to  $\text{TiO}_2$ -EG and  $\text{CuO}$ -EG because of the marginal difference in the values of the thermal conductivities (0.3% higher as compared to  $\text{TiO}_2$ -EG nanofluid and 0.2% as compared to  $\text{CuO}$ -EG nanofluid). For higher nanoparticle concentration ( $\phi_b = 10\%$ ), the  $T_w$  decreases by 15 K for the  $\text{Al}_2\text{O}_3$ -EG nanofluid due to the movement of nanoparticles at a higher Re, which results in a higher thermal efficiency.

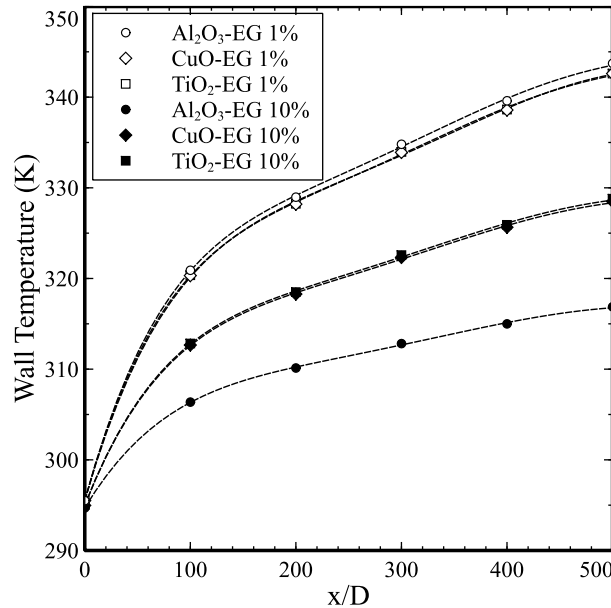


**Figure 13.** Effect of nanoparticle concentration in tube flow: axial development of wall temperatures.

## 4.3 Case 3: Oil nanofluid in st. tube with constant heat flux using SPH

Case 3 considers oil-based nanofluids with the same parameters used in previous two cases. The effect of base fluid was investigated using three different base fluids viz. water, ethylene glycol and oil with the same nanoparticle ( $\text{Al}_2\text{O}_3$ ,  $\phi_b = 4\%$ ) as shown in Figure 14.

All the nanofluids (Al<sub>2</sub>O<sub>3</sub>-water, Al<sub>2</sub>O<sub>3</sub>-EG and Al<sub>2</sub>O<sub>3</sub>-oil) significantly enhance the value of Nu as compared to the any base fluid alone. It may be noted that the Nu enhanced by 16% for Al<sub>2</sub>O<sub>3</sub>-water nanofluid as compared to the water, 12% for the Al<sub>2</sub>O<sub>3</sub>-EG nanofluid as compared to ethylene glycol and 8% for the Al<sub>2</sub>O<sub>3</sub>-oil when compared to oil. The Nu enhancement is due to similar reasons as previous two cases.

The heat transfer enhancement using nanofluids may be affected by several factors such as gravity, Brownian motion, Brownian diffusion, friction force between the fluid and nanoparticles, sedimentation, dispersion, layering at the solid/liquid interface, ballistic phono transport and thermophoresis may coexist in the main flow of a nanofluid. Particle fluctuations and interaction, especially in high Peclet number may cause the change in flow structure and lead to augmented heat transfer due to the presence of nanoparticles. Because of the effects of several factors, the heat characteristics of nanofluids are dependent on the properties of the base liquid and the dispersed phases, particle concentration, size and morphology, as well as the presence of dispersants or surfactants. Therefore, the general form of the Nusselt number yields:  $Nu = f(Re, Pr, \phi_b)$ . This general form can also include particle size and shape and flow structure. For this study, the Nusselt number form was considered to be:  $Nu = f(Re, Pr)$  as the main intention is to determine the enhancement of different nanofluids and not the nanoparticles itself (size and shape).

A new correlation for Nu (eq. 41) has been developed covering a wide range of the nanoparticle concentration ( $0\% \leq \phi_b \leq 10\%$ ) and Prandtl number (6.0 – 500) under the constant heat flow and laminar flow conditions ( $25 < Re < 1500$ ). Figure 15 shows the comparison between the present computed Nu results, the experimental results and the computed data from the literature with the present proposed correlation (eq. 41). It may be observed from Figure 15, that the present results of Nu are in good agreement with the experimental results (variation of  $\pm 5\%$ , 4.8% absolute difference) developed by Wen & Ding [17], Anoop et al. [20], Heris et al. [44], Heris et al. [47] and with computational results from Maïga et al. [7].

$$Nu = 0.4381Re^{0.36}Pr^{0.42} \quad (41)$$

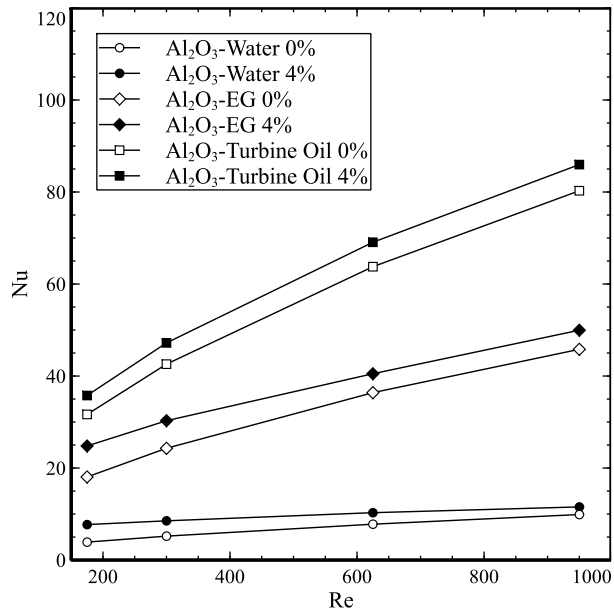


Figure 14. Comparison of Nu for Al<sub>2</sub>O<sub>3</sub>-water, Al<sub>2</sub>O<sub>3</sub>-EG and Al<sub>2</sub>O<sub>3</sub>-oil at  $\phi_b = 4\%$ .

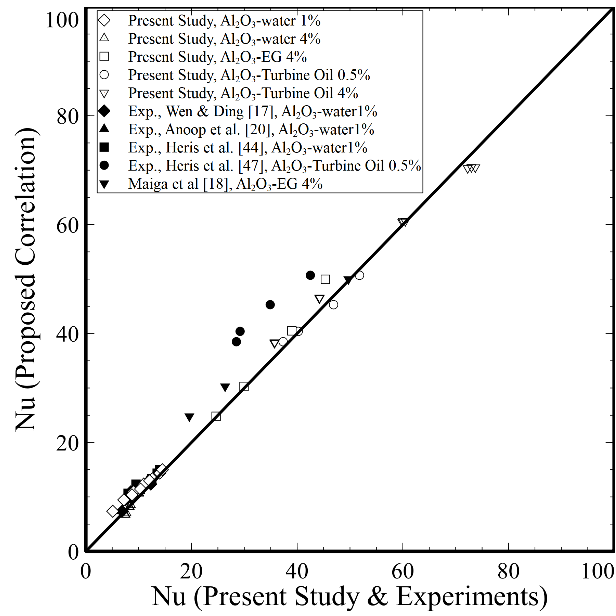
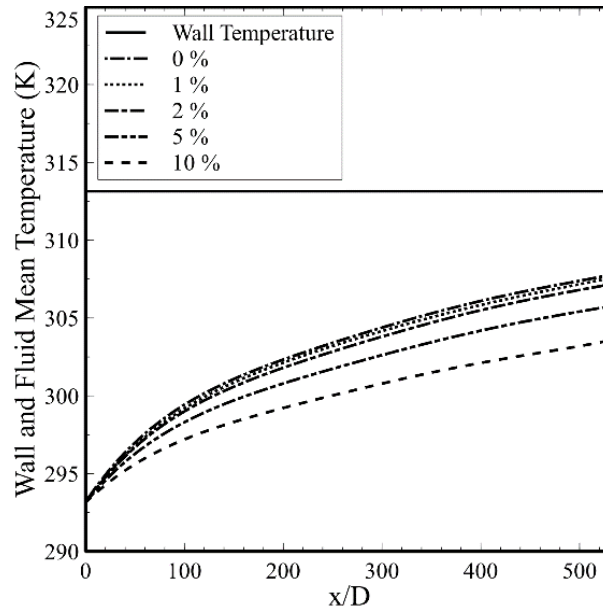


Figure 15. Proposed correlation vs computed results and experiments of Nu in a straight tube.

#### 4.4 Case 4: Water nanofluid in st. tube with constant wall temperature using SPH

In this case water-based nanofluids are used at a constant wall temperature ( $T_w = 313.15$  K) condition with an inlet fluid temperature of  $T_o = 293.15$  K, at  $Re = 500$ . Figure 16 demonstrates the effect of the nanoparticle concentration on the  $T_m$  for constant wall temperature condition.



**Figure 16.** Effect of nanoparticle concentration in tube flow: axial development of wall and  $T_m$ .

It can be observed that the  $T_m$  decreases with increase in the concentration of nanoparticles due to the improved heat capacity (up to 23%). The  $T_m$  for a highest nanoparticle concentration ( $\phi_b = 10\%$ ) was lower by 10 K as compared to the water. The diminution of temperature reflects the improvement in the thermal properties of the resulting mixture caused by the Brownian motion. The effect of the different water based nanofluids was investigated using different nanoparticles viz  $Al_2O_3$ ,  $TiO_2$ ,  $CuO$ ,  $SiO_2$  and  $ZnO$ , as shown in Figure 17. It may be noted that the  $Al_2O_3$ -water nanofluid has a higher heat transfer rate than all other nanofluids. The enhancement in  $Nu$  for the  $Al_2O_3$ -water is 14% higher as compared to  $ZnO$ -water nanofluid.

Figure 18 shows the overall effect of the different base fluids on Nu for constant temperature boundary condition. The Nu at Re = 950 enhanced by 16% for Al<sub>2</sub>O<sub>3</sub>-water nanofluid as compared to water, 10% for Al<sub>2</sub>O<sub>3</sub>-EG nanofluid as compared to ethylene glycol and 8% for Al<sub>2</sub>O<sub>3</sub>-oil nanofluid as compared to oil. The enhancement in the Nu is mainly due to the thermophysical properties of the nanoparticles.

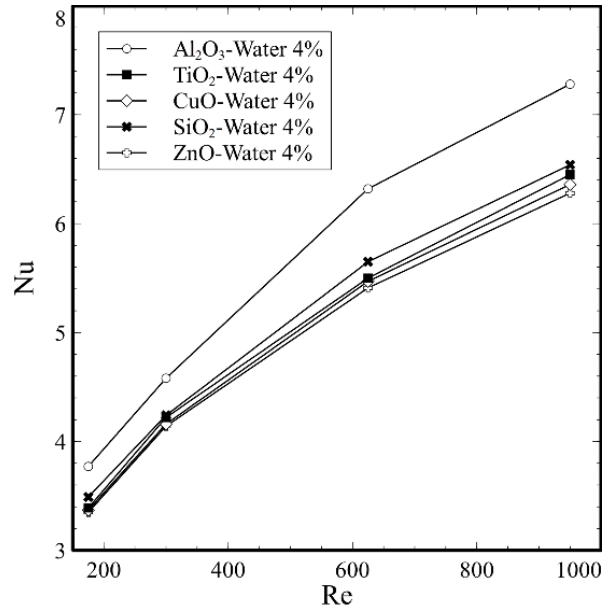


**Figure 17.** Comparison of Nu for Al<sub>2</sub>O<sub>3</sub>-water, TiO<sub>2</sub>-water, CuO-water, SiO<sub>2</sub>-water and ZnO-water and at  $\phi_b = 4\%$ .

For the average Nu in a straight tube with constant wall temperature a new correlation (eq. 42) is proposed by fitting the data obtained from the numerical simulations. The correlation covers a wide range of the nanoparticle concentration ( $0\% \leq \phi_b \leq 10\%$ ) and Prandtl number (6.0 – 500) under the laminar flow condition ( $25 < Re < 1500$ ).

Figure 19 shows the comparison between the present computed Nu results, with the experimental results from the Heris et al. [8] and the computed data from Maïga et al. [18] with the present proposed correlation (eq. 42). A good agreement was attained between the computed and previous experimental work with the predicted values of the Nu with a variation of  $\pm 5\%$  (5.5% absolute difference).

$$Nu = 0.257Re^{0.37}Pr^{0.36} \quad (42)$$



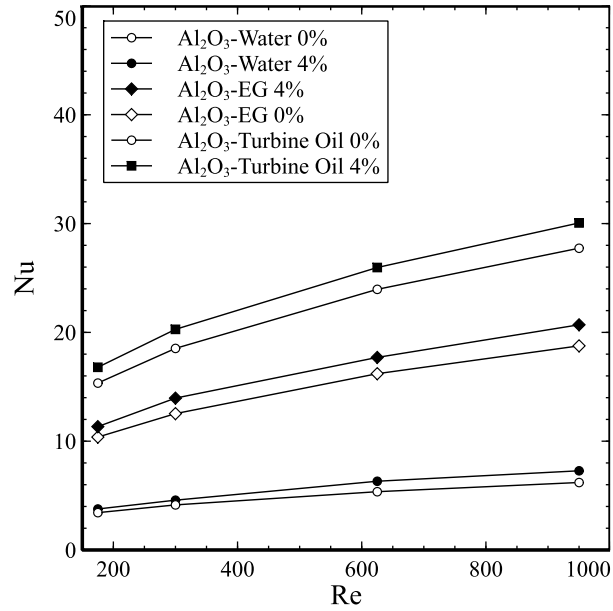


Figure 18. Comparison of Nu for Al<sub>2</sub>O<sub>3</sub>-water, Al<sub>2</sub>O<sub>3</sub>-EG and Al<sub>2</sub>O<sub>3</sub>-oil at  $\phi_b = 4\%$ .

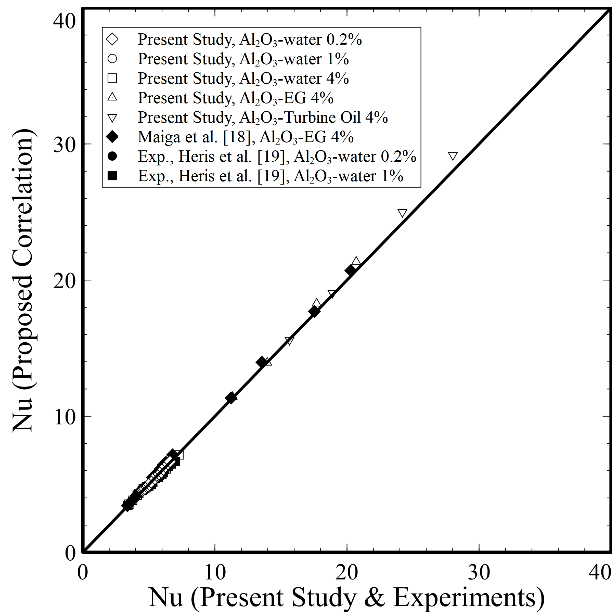
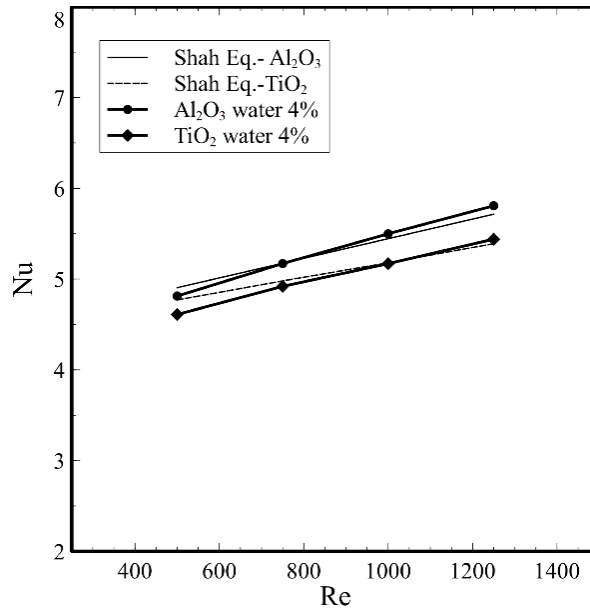


Figure 19. Proposed correlation vs computed results and experiments of Nu in a straight tube.

#### 4.5 Case 5: Water-based nanofluid in st. microtube with constant heat flux using SPH

In case 5, all the different nanofluids Al<sub>2</sub>O<sub>3</sub>-water, TiO<sub>2</sub>-water, CuO-water, SiO<sub>2</sub>-water and ZnO-water are used to investigate the Nu in a straight microtube with a length of 0.3 m and an inner diameter ( $d_t$ ) of 0.5 mm. Results from the numerical simulation were compared with Shah's [34] correlation (eq. 43) for validation purpose. A good agreement can be seen in between the present computed results of Nu with the predicted values from Shah's correlation, as shown in Figure 20.

$$Nu = \begin{cases} 1.953 \left( RePr \frac{D}{L} \right)^{\frac{1}{3}} & RePr \frac{D}{L} \geq 33.3 \\ 4.364 + 0.0722 RePr \frac{D}{L} & RePr \frac{D}{L} < 33.3 \end{cases} \quad (43)$$



**Figure 20.** Comparison of Nu with literature: Al<sub>2</sub>O<sub>3</sub>-water nanofluid at  $\phi_b = 4\%$ .

It may be noted from Figure 21a and Figure 21b, that similar to the straight tube results, the wall temperature as well as fluid mean temperature in the straight microtube also decreases with increase in the nanoparticle concentration. The decrease in the temperatures of the wall and the fluid will result in a better heat transfer.

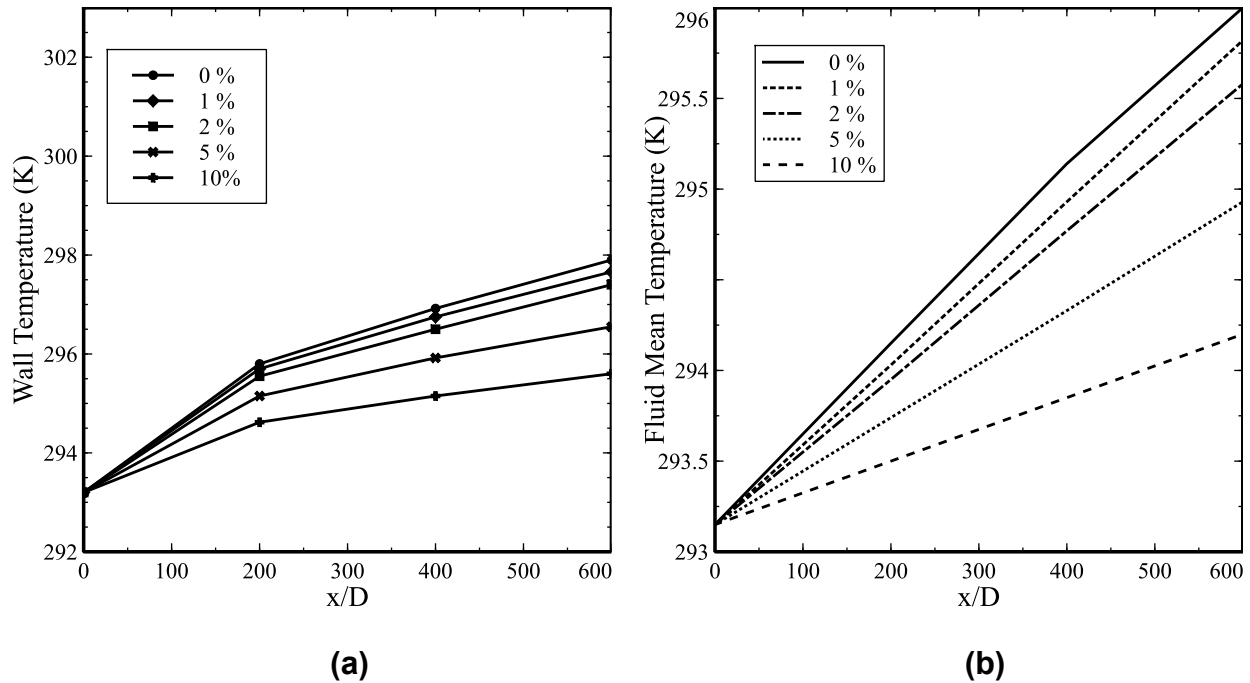


**Figure 21.** Effect of nanoparticle concentration in tube flow: (a) axial development of wall temperatures, (b) fluid mean temperatures for Al<sub>2</sub>O<sub>3</sub>-water.

Figure 22 shows the effect of the different type of nanoparticles for a water-based nanofluid. The Al<sub>2</sub>O<sub>3</sub>-water nanofluid has a better heat transfer enhancement as compared to that of all the other nanoparticles due to the higher thermal conductivity. Figure 23 shows the Nu for different fluids at the same Re = 950. The oil-based nanofluid has the higher Nu, however it is not the nanofluid with the higher enhancement. The Nu enhancement was 6% for Al<sub>2</sub>O<sub>3</sub>-water compared to water, 12% for Al<sub>2</sub>O<sub>3</sub>-EG compared to ethylene glycol and 5% for Al<sub>2</sub>O<sub>3</sub>-oil compared to oil. Based on this results it may be concluded, that ethylene glycol-based nanofluids are the best choice for heat transfer enhancement at the same Re and  $\phi_b$ . The hydrodynamics play an important role in determining the thermal performance of any heat transfer device. It is noteworthy, that the scale has a significant effect on the heat transfer performance. The conventional straight tube provides higher heat transfer performance as compared to straight microtube. It may be noted that the Nusselt got enhanced 16% for Al<sub>2</sub>O<sub>3</sub>-water in comparison with 6% for Al<sub>2</sub>O<sub>3</sub>-water for a straight tube and straight microtube, respectively, when compared to water ( $\phi_b = 4\%$ ).

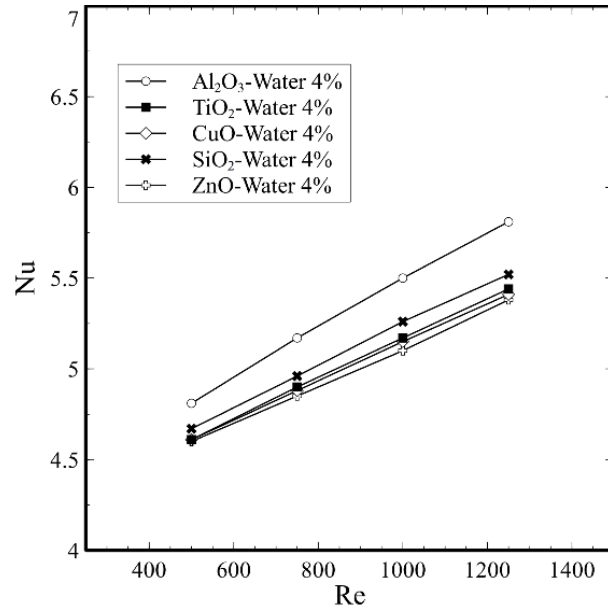


Figure 22. Comparison of Nu for water-based nanofluids at  $\phi_b = 4\%$ .

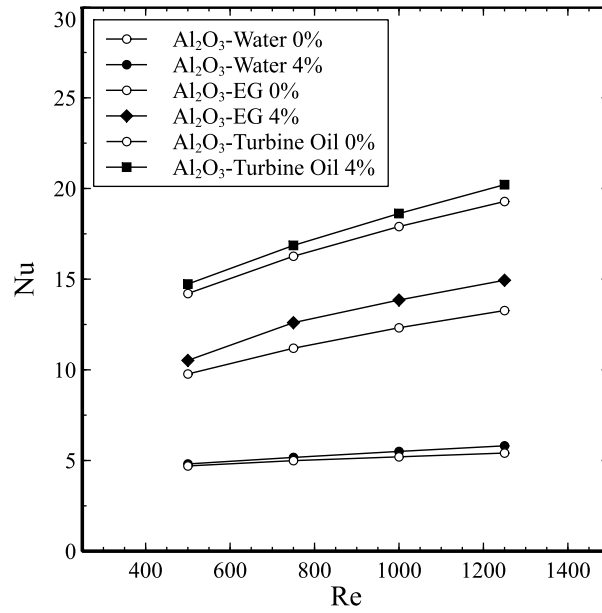
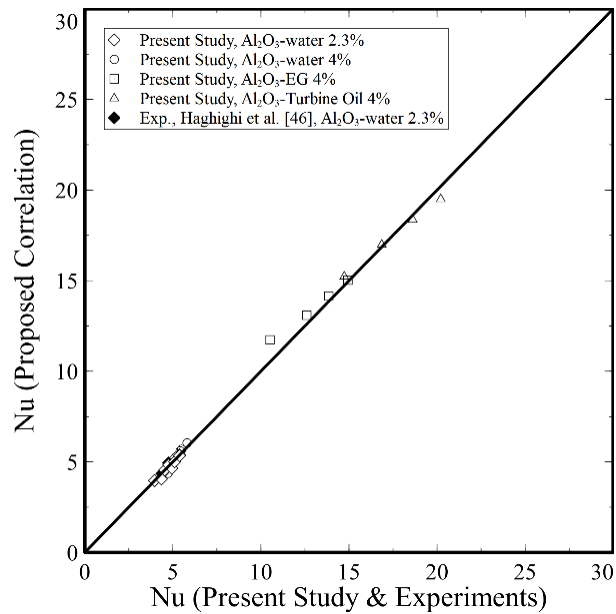


Figure 23. Comparison of Nu for Al<sub>2</sub>O<sub>3</sub>-water, Al<sub>2</sub>O<sub>3</sub>-EG and Al<sub>2</sub>O<sub>3</sub>-oil at  $\phi_b = 4\%$ .

For the average Nu in a microtube with constant heat flux a new correlation (eq. 38) is proposed by fitting the data obtained from the numerical simulations. The correlation covers a wide range of the process parameters ( $25 < Re < 1500$ ,  $0 < \phi_b < 10$ ,  $6 < Pr < 500$ ) under the laminar flow condition.

Figure 24 shows the comparison between the present Nu results along with the experiments from Haghghi et al. [46] with the present proposed correlation (eq. 44). The predicted values of Nu are in good agreement (variation of  $\pm 5\%$  or a 3.2% absolute difference) with the computed values and the previous experimental results.

$$Nu = 0.4561Re^{0.27}Pr^{0.30} \quad (44)$$



**Figure 24.** Proposed correlation vs computed results and experiments of Nu in a straight tube.

#### 4.6 Case 6: Water-based nanofluid in st. tube with constant heat flux using SPD

Case 6 purpose is to simulate the nanofluid flow for a constant heat flux condition in a straight tube using the SPD. Figure 25 shows a comparison of the computed Nu results using SPD and SPH. It may be noted that the Nu increases with the increase of the Re.

The SPD shows a higher Nu due to a higher thermal conductivity and viscosity of the nanofluid. Results of the SPD model show agreement with Liu et al. [27], where the Nu of the nanofluid is better predicted in the SPD than in the SPH. The SPD model is recommended as the appropriate model for predicting heat transfer characteristic of nanofluid flow in a straight tube.

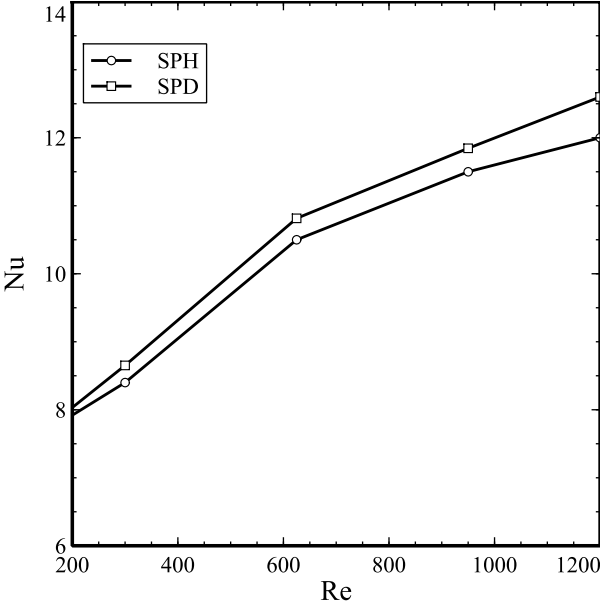


**Figure 25.** Comparison of Nu with literature: Al<sub>2</sub>O<sub>3</sub>-water nanofluid at  $\phi_b = 4\%$  for SPH and SPD.

## Chapter

### 5 Conclusions & Recommendations

#### 5.1 Conclusions

In the present study, heat transfer of different nanofluid types were investigated using two configurations: straight tube and straight microtube. Both geometries presented an enhancement in the Nu using nanofluid. In case of the straight tube with  $\phi_b = 4\%$ , the Nu increases 16% for Al<sub>2</sub>O<sub>3</sub>-water as compared to water, 12% for Al<sub>2</sub>O<sub>3</sub>-EG as compared to EG and 8% for Al<sub>2</sub>O<sub>3</sub>-oil as compared to oil. For the straight microtube with  $\phi_b = 4\%$  the Nu increases 6% for Al<sub>2</sub>O<sub>3</sub>-water as compared to water, 12% for Al<sub>2</sub>O<sub>3</sub>-EG as compared to ethylene glycol and 5% for Al<sub>2</sub>O<sub>3</sub>-oil as compared to oil.

Despite the better heat transfer enhancement in Al<sub>2</sub>O<sub>3</sub>-EG and Al<sub>2</sub>O<sub>3</sub>-oil it is important to consider the associated higher values of the wall shear stress (e.g. quadruple of the corresponding based fluid for an Al<sub>2</sub>O<sub>3</sub>-EG nanofluid with high nanoparticle concentration  $\phi_b = 10\%$ ) and that the effect of the surfactants or dispersant agents was not included, so without these special treatments, the nanoparticles would agglomerate causing a reduction in thermal conductivity of the nanofluids. The comparison between the different nanoparticles viz. Al<sub>2</sub>O<sub>3</sub>, TiO<sub>2</sub>, CuO, SiO<sub>2</sub> and ZnO revealed that the Al<sub>2</sub>O<sub>3</sub> nanoparticle with the three based fluids (water, ethylene glycol and oil) has a higher Nu due to the higher thermal capacity. The present results clearly showed that the addition of nanoparticles increases the Nu up to 16 % as compared to the base fluid. For all the cases, the Nu enhancement becomes more pronounced due to nanoparticles.

Two different boundary conditions were considered (constant heat flux and constant temperature), and thus two new convective heat transfer correlations were proposed for the straight tube covering a wide range of the process parameters ( $25 < Re < 1500$ ,  $0 < \phi_b < 10$ ,  $6 < Pr < 500$ ) under laminar flow condition. Also, a new Nu correlation for the straight microtube was proposed for the same range of process parameters to that of straight tube. This correlations fairly matches with the values of experimental studies and cover most applications, however there is a strong influence of particle properties and nanofluid composition on flow and heat transfer characteristics.

## 5.2 Main contributions

This study was conducted to determine the effect in the convective heat transfer in nanofluids for a straight tube and straight microtube. In order to determine this effect different metallic nanoparticles ( $\text{Al}_2\text{O}_3$ ,  $\text{TiO}_2$ ,  $\text{CuO}$ ,  $\text{SiO}_2$  and  $\text{ZnO}$ ), different base fluids (water, ethylene glycol and oil) and boundary conditions (uniform heat flux and uniform surface temperature) were used. This process parameters were carefully selected to cover a wide range and solved using single phase and single-phase dispersion numerical models. From this considerations, the main contributions of this investigation are the following:

- Heat transfer correlations for the flow of nanofluids over a wide range of process conditions ( $25 < \text{Re} < 1500$ ,  $0 < \phi_b < 10$ ,  $6 < \text{Pr} < 500$ ) for:
  - Conventional straight tube under constant heat flux:  
$$\text{Nu} = 0.4381 \text{Re}^{0.36} \text{Pr}^{0.42}$$
  - Conventional straight tube under constant temperature:  
$$\text{Nu} = 0.257 \text{Re}^{0.37} \text{Pr}^{0.36}$$
  - Conventional straight microtube under constant heat flux:  
$$\text{Nu} = 0.4561 \text{Re}^{0.27} \text{Pr}^{0.30}$$
- Identification of the Nusselt number improvements from three different type of based fluids including water, ethylene glycol and oil with five different type of nanoparticles viz.  $\text{Al}_2\text{O}_3$ ,  $\text{TiO}_2$ ,  $\text{CuO}$ ,  $\text{SiO}_2$  and  $\text{ZnO}$ .
- Demonstration that the addition of nanoparticles clearly showed an increase of the Nusselt number as compared to the base fluids. For all the cases considered in the study, the Nu enhancement becomes more pronounced due to nanoparticles.



### 5.3 Recommendations

The recommendations for future work are:

- Continue exploring different nanoparticles (metallic) and consider different aspects such as: size (20-100 nm) and shape (spherical, disk shape or cylindrical). During the literature review some articles are adding complexity by determining experimentally or numerically the effect in convective heat transfer by considering the nanoparticles size and shape. It was identified that there is no general correlation due to lack of common understanding on mechanism of nanofluid.
- Considered the new complex geometries such as helical tube and coiled flow inverter tube. Geometry perturbation is a well-established technology to improve the fluid phenomena and heat transfer as reported in the literature. Adding different geometric configurations will allow to identify the effect on the heat transfer performance due to the geometry perturbation. Nowadays, industrial applications are using heat exchangers with this type of tubes which will further extend what was explored in this study.
- Analyze the different numerical models such as the two-phase models. In the two-phase model the nanoparticle and the base fluid are considered as two different phases with different velocities and temperatures. By using this model, it could be possible to determine the effect of the nanoparticles on the velocity and temperature field.
- Perform additional experiments to validate the numerical results to provide greater certainty. Currently, due to the limitations in the experiments it will be attractive to validate some of the calculated convective heat transfer enhancements, especially, for the ranges that are currently not covered by the available literature. Additionally, testing and validating the nanofluids to identify the thermodynamic properties will be important as they are a relevant input in the numerical calculations and simulations.
- Continue the study of different mechanisms of the nanofluids, specially the Brownian motion. The Brownian motion which can be studied numerically by using the dynamic single-phase model considers the effect of this motion on the thermal conductivity and viscosity.

## Appendix A

### Abbreviations and Symbols

---

Abbreviations	
Al <sub>2</sub> O <sub>3</sub>	Aluminum Oxide
CFD	Computational Fluid Dynamics
CuO	Copper Oxide
HTC	Heat Transfer Coefficient
SiO <sub>2</sub>	Silicon Dioxide
SPD	Single Phase Dispersion Model
SPH	Single Phase Model
TiO <sub>2</sub>	Titanium Dioxide
ZnO	Zinc Oxide

---

Symbols	
$C_p$	Specific Heat Capacity
$c_{eff}$	Specific Heat Capacity of Nanofluid
$d_t$	Tube Inner Diameter
$k_{eff}$	Effective Thermal Conductivity of Nanofluid
$k_{disp}$	Dispersion Thermal Conductivity
$L$	Length of the Tube
$\mu_{eff}$	Effective Viscosity of Nanofluid
$\mu_{disp}$	Dispersion Viscosity
$\phi_b$	Volume Fraction of Nanoparticles
$\rho_{eff}$	Density of Nanofluid
Pr	Prandtl Number
Nu	Nusselt Number
Re	Reynolds Number
$T_o$	Initial Temperature
$T_m$	Fluid Mean Temperature
$U$	Mean Velocity of Nanofluid

---

## Appendix B

### Experimental and numerical studies

**Table B. 1** Experimental and numerical studies for forced convective heat transfer of nanofluids for laminar flow.

Author	Type of study	Nanofluid	Boundary Condition	Particle loading (vol%)	Flow Regime	Type of heat exchanger	Results
Wen & Ding [17]	Experimental	$\gamma$ -Alumina/water	Constant $\dot{Q}$	0.6, 1 & 1.6	Laminar 500 – 2100	Straight Tube	Local HTC enhancement of 47%
Maïga et al. [18]	Experimental	$\gamma$ -Alumina/water, $\gamma$ -Alumina/ Ethylene Glycol	Constant $\dot{Q}$ Constant $T_w$	0 – 10	Laminar 250 -1000	Straight Tube	HTC enhancement of 63% for 7.5 vol% particle loading, Re = 1000 $Nu_{nf} = 0.086Re_{nf}^{0.55}Pr_{nf}^{0.5}$ for Constant $\dot{Q}$ $Nu_{nf} = 0.28Re_{nf}^{0.35}Pr_{nf}^{0.36}$ for Constant $T_w$
Heris et al. [19]	Experimental	CuO/water, Alumina/water	Constant $T_w$	0.2 – 3	Laminar 650 – 2050	Straight Tube	HTC increases with decrease in particle size and increase in particle loading
Anoop et al. [20]	Experimental	Alumina/water	Constant $\dot{Q}$	1 – 6	Laminar 500 – 2000	Straight Tube	Enhancement in HTC was around 25% for 4 wt%. $Nu_x = 4.36 + [ax_+^{-b}(1 + \phi^c)exp^{-dx_+}] \left[ 1 + e \left( \frac{d_p}{d_{ref}} \right)^{-f} \right] 6.219 \times 10^{-3}$ , b=1.1522, c=0.1533, d=2.5228, e=0.57825, f=0.2183, $d_{ref}=100$ nm, $x_+=x/(DRePr)$
Hwang et al. [21]	Experimental	Alumina/water	Constant $\dot{Q}$	0.01-0.3	Fully Dev. 500 - 800	Straight Tube	HTC is increased by 8% at 0.3 vol% under fixed Reynolds number
Davarnejad et al. [22]	Numerical	Alumina/water	Constant $\dot{Q}$	0.5 – 2.5	Laminar 420–990	Straight Tube	HTC increases by increasing velocity and decreasing the particle diameter
Kim et al. [23]	Experimental	Alumina/water Amorphous carbonic nanoparticles/ water	Constant $\dot{Q}$	0-3	Laminar 800 – 2400	Straight Tube	Alumina nanofluids containing 3 vol% had a 8% increment of thermal conductivity

Author	Type of study	Nanofluid	Boundary Condition	Particle loading (vol%)	Flow Regime	Type of heat exchanger	Results
Purohit et al. [25]	Numerical	Alumina, Zirconia & Titanate/water	Constant $\dot{Q}$	0.5 – 2	Laminar 1150–1900	Straight Tube	HTC enhancement reaches a maximum of 18%
Purohit et al. [25]	Numerical	Alumina, Zirconia & Titanate/water	Constant $\dot{Q}$	0.5 – 2	Laminar 1150–1900	Straight Tube	HTC enhancement reaches a maximum of 18%
Haghighi et al. [26]	Experimental	Alumina, Zirconia & Titanate/water	Constant $\dot{Q}$	9	Laminar 10 - 2300	Straight Tube	HTC increases a maximum of 23%
Singh et al. [43]	Numerical	Al <sub>2</sub> O <sub>3</sub> -water TiO <sub>2</sub> -water	Constant $\dot{Q}$	1 -4 %	Laminar	Straigh Tube	Nu in helical coil augments 2.5 of that of straight tube. In CFI, the Nu further enhanced by 23-35% as compared to helical coil
Bianco et al. [48]	Numerical	Alumina/water	Constant $\dot{Q}$	1, 4	Laminar	Straight Tube	HTC was increasing with the concentration of particle volume
Behzadmehr et al. [49]	Numerical	Alumina/water	Constant $\dot{Q}$	0 – 2	Laminar	Straight Tube	HTC increases by 11% when Re increases from 1050 to 1600
Ting et al. [52]	Numerical	Alumina/water	Constant $T_w$	0 – 2	Laminar	Straight Tube	HTC with 2 vol.% Al <sub>2</sub> O <sub>3</sub> nanoparticles is enhanced by 32%
Fard et al. [53]d	Numerical	Cu/water	Constant $T_w$	0.2	Laminar	Straight Tube	HTC increases with Peclet Number
Arzani et al. [54]	Numerical	CuO/water	Constant $\dot{Q}$	0 – 8	Laminar	Straight Tube w/180° curve	With the increase of volume fraction , the Nu of the nanofluid increases
Kristiawan et al. [55]	Numerical	TiO <sub>2</sub> /water	Constant $\dot{Q}$	0.24 – 1.18	Laminar	Straight Tube	Results validated with the Shah and London equation
Li & Xuan [81]	Experimental	Cu/water	Constant $\dot{Q}$	0.5 – 2	Laminar 800 – 2100	Straight Tube	Heat transfer coefficient increases to max 60% with 2.0 vol.% Cu. $Nu_{nf} = 0.4328(1 + 11.258\phi^{0.754} Pe_p^{0.218}) Re_{nf}^{0.333} Pr_{nf}^{0.4}$

## Bibliography

- [1] Pawar, S.S.; Nandi, S.; Salian, T.; Shenoy, G.; Shetty, S. A brief review on CFD work of helical coil and straight tube heat exchangers. *Int. J. Phys. Appl. Sci.* **2015**, 2, 11.
- [2] Das, S.K., Choi, S.U.S., Yu, W., Pradeep, T. *Nanofluids: Science and Technology*, John Wiley & Sons, **2007**.
- [3] Wang, L., and Fan, J. Nanofluids research: Key Issues. *Nanoscale Res. Lett.* 5, no. 8, **2010**: 1241-1252.
- [4] Sen, M., and Paolucci, S. The use of ionic liquids in refrigeration. Paper No. IMECE 2006-14712. ASME International Mechanical Engineering Congress and Exposition Proceedings. Chicago, IL., **2006**. 131-134.
- [5] Masuda, H., Ebata, A., Terama, K., Hishinuma, N. Alteration of thermal conductivity and viscosity of liquid by dispersing ultra-fine particles (dispersion of  $\gamma$ -Al<sub>2</sub>O<sub>3</sub>, SiO<sub>2</sub>, and TiO<sub>2</sub> ultra-fine particles. *Jpn. J. Thermophys. Prop.* 7, no. 4, **1993**: 227-233.
- [6] Das, S.K., Putra, N., Thiesen, P., Roetzel, W. Temperature dependence of thermal conductivity enhancement for nanofluids. *J. Heat Transf.* 125, no. 4, **2003**: 567-574.
- [7] Putman, S.A., Cahill, D.G., Braun, P.V., Ge, Z., Shimmin, R.G. Thermal conductivity of nanoparticle suspensions. *J. Appl. Phys.* 99, no. 8, **2006**: 084308.
- [8] Wang, Z. Thermal wave in thermal properties measurements and flow diagnostics: With applications of nanofluids thermal conductivity and wall shear stress measurements. PhD dissertation, Oregon State University, Corvallis, OR, **2009**.
- [9] Pak, B.C. and Cho, Y.I. Hydrodynamic and heat transfer study of dispersed fluids with submicron metallic oxide particles. *Exp. Heat Transf.* 11, no. 2, **1998**: 151-170.
- [10] Namburu, P.K., Kulkarni, D.P., Misra, D., Das, D.K. Viscosity of copper oxide nanoparticles dispersed in ethylene glycol and water mixture. *Exp. Therm. Fluid Sci.* 32, no. 2, **2007**: 397-402.
- [11] Bergman, T. Effect of reduced specific heats of nanofluids on single phase, laminar internal forced convection. *Int. J. Heat Mass Transf.* 52, no. 5-6, **2009**: 1240-1244.
- [12] Shin, D., Banerjee, D. Enhancement of specific heat capacity of high-temperature silica-nanofluids synthesized in alkali chloride salt eutectics for solar thermal-energy storage applications. *Int. J. Heat Mass Transf.* 54, no. 5-6, **2011a**: 1064-1070.
- [13] Sunny, S.P.; Mhaske, S.D.; Parikh, Y.B. Numerical Simulation of a Tube in Tube Helical Coiled Heat Exchanger using CFD. *Int. J. of Applied Eng. Research.* **2014**, 9, 18.
- [14] Gupta, M.; Arora, N.; Kumar, R.; Kumar, S.; Dilbaghi, N. A comprehensive review of experimental investigations of forced convective heat transfer characteristics for various nanofluids. *Int. J. of Mechanical and Materials Eng.* **2014**, 9, 11.
- [15] Akbaridoust, F.; Rakhsha, M.; Abbassi, A.; Saffar-Avval, M. Experimental and numerical investigation of nanofluid heat transfer in helically coiled tubes at constant wall temperature using dispersion model. *Int. J. of Heat and Mass Transfer.* **2013**, 58, 480-491.
- [16] Shokouhi, A.; Keshazarz, A.; Ziabasharhagh, M.; Mojarrad, M.S.; Raveshi, M.R. Experimental Investigation of Nanofluid Convective Heat Transfer in the Entrance Region of a Circular Tube. *MNHMT* **2012**-75253.

- [17] Wen, D.; Ding, Y. Experimental investigation into convective heat transfer of nanofluids at the entrance region under laminar flow conditions. *Int. J. of Heat and Mass Transfer*. **2004**, 47, 5181-5188.
- [18] Maïga, S.E.B.; Palm, S.J.; Nguyen, C.T.; Roy, G.; Galanis, N. Heat transfer enhancement by using nanofluids in forced convection flows. *Int. J. Heat Fluid Flow*. **2005**, 26(4), 530-546.
- [19] Heris, S.Z.; Etemad, S.G.; Esfahany, M.N. Experimental investigation of oxide nanofluids laminar flow convective heat transfer. *Int. Commun. Heat Mass Transfer*. **2006**, 33 (49), 529 – 535.
- [20] Anoop, K.B.; Sundararajan, T.; Das, S.K. Effect of particle size on the convective heat transfer in nanofluid in the developing region. *Int. J. of Heat and Mass Transfer*. **2009**, 52 (9-10), 2189 – 2195.
- [21] Hwang, K.S.; Jang, S.P.; Choi, S. Flow & convective heat transfer characteristics of water-based Al<sub>2</sub>O<sub>3</sub> nanofluids in fully developed laminar flow regime. *Int. J. of Heat and Mass Transfer*. **2009**, 52 (1-2), 193-199.
- [22] Davarnejad, R.; Barati, S.; Kooshki, M. CFD simulation of the effect of particle size on the nanofluids convective heat transfer in the developed region in a circular tube. *Springer Plus*. **2013**, 2(1), 1-6.
- [23] Kim, D.; Kwon, Y.; Cho, Y.; Moon, S. Convective heat transfer characteristics of nanofluids under laminar and turbulent flow conditions. *Current Applied Physics*. **2009**, 9, 119-123.
- [24] Rea, U.L.; McKrell, T.; Hu, L. Laminar convective heat transfer and viscous pressure loss of alumina–water and zirconia–water nanofluids. *Int. J. of Heat and Mass Transfer*. **2009**, 52, 2042-2048.
- [25] Purohit, N; Purohit, V.A.; Purohit, K. Assessment of nanofluids for laminar convective heat transfer: A numerical study. *Eng. Science and Tech an Int. Journal*. **2016**, 19, 574-586.
- [26] Haghghi, E.B.; Saleemi, M.; Nikkam, N.; Khodabandeh, R.; Toprak, M.S.; Muhammed, M.; Palm, B. Accurate basis of comparison for convective heat transfer in nanofluids. *Int. Commun. Heat Mass Transfer*. **2014**, 52, 1-7.
- [27] Liu, Y.; Hu, H. Numerical investigation of nanofluid convection performance in the fully developed flow regime of the pipe with constant wall temperature. *IOP Conference Series: Earth and Environmental Science*. **2017**, Volume 59, Conference 1.
- [28] Göktepe, S.; Atalik, K.; Ertürk, H. Comparison of single and two-phase models for nanofluid convection at the entrance of a uniformly heated tube. *Int. J. of Thermal Sciences*. **2014**, 80, 83-92.
- [29] Wang, X.Q.; Mujumdar, A. S. A review on nanofluids – Part I: Theoretical and numerical investigations. *Brazilian J. of Chemical Eng.* **2008**, Vol- 25, No.04, 613-630.
- [30] Pak, B.C.; Cho, Y.I. Hydrodynamic and heat transfer study of dispersed fluids with submicron metallic oxide particles. *Exp. Heat Transfer*. **1999**, 11, 151-170.
- [31] Ho, C.J.; Liu, W.K.; Chang, Y.S.; Lin, C.C. Natural convection of microparticle suspensions in thin enclosures, *Int. J. of Heat and Mass Transfer*. **2008**, 51, 1332 – 1341.

- [32] Das, S.K.; Putra, N.; Thiesen, P.; Roetzzel, W. Temperature dependence of thermal conductivity enhancement for nanofluids. *J. Heat Transfer*. **2003**, 125, 567-574.
- [33] Khanafer, K.; Vafai, K. A critical synthesis of thermophysical characteristics of nanofluids. *Int. J. of Heat & Mass Transfer*, **2011**, 54, 4410 – 4428.
- [34] Brinkman, H.C. The viscosity of concentrated suspensions and solutions. *Journal Chem. Phys.* **1952**, 20.
- [35] Lundgren, T. Slow flow through stationary random beds and suspensions of spheres. *J. Fluid Mech.* **1972**, 51, 273-299.
- [36] Batchelor, G. The effect of Brownian motion on the bulk stress in a suspension of spherical particles. *J. Fluid Mech.* **1977**, 83, 97 – 117.
- [37] Hamilton, R.L.; Crosser, O.K. Thermal Conductivity of heterogeneous two-component systems. *I&EC Fundam.* 1. **1962**, 182- 191.
- [38] Maxwell, J.C.A. *Treatise on Electricity and Magnetism*, Second Edition, Clarendon Press, Oxford, UK, **1881**.
- [39] Buongiorno J.; Venerus, D.C.; McKrell, T.; Townsend, J. A Benchmark Study on the Thermal Conductivity of Nanofluids. *J. Appl. Phys.* **2009**, 106(9), 094312.
- [40] Sarkar, J. A critical review on convective heat transfer correlations of nanofluids. *Renewable and Sustainable Energy Reviews*. **2011**, 15, 3271-3277.
- [41] Tertsinidou, G.J.; Tsolakidou, C.M.; Pantzali, M.; Assael, M.J. New Measurements of the Apparent Thermal Conductivity of Nanofluids and Investigation of Their Heat Transfer Capabilities. *J of Chemical & Eng. Data*. **2017**, 62(1), 491-507.
- [42] Heris, S.Z.; Shokrgozar, M., Poorpahrhang, S., Shanbedi, M., Noie, S. Experimental study of heat transfer of a car radiator with CuO/ethylene glycol-water as a coolant. *J. of dispersion science and technology*. **2014**, 35, 677-684.
- [43] Singh, J.; Choudhary, N.; Nigam, K.D.P. The Thermal and Transport Characteristics of Nanofluids in a Novel Three-Dimensional Device, *Canadian J. of Chemical Engineering*. **2014**, 94, 2185-2201.
- [44] Heris, S.Z.; Etemad, S.G.; Esfahany, M.N. Experimental investigation of convective heat transfer for Al<sub>2</sub>O<sub>3</sub>/water nanofluid in circular tube. *Int. J. of Heat and Fluid Flow* **2007**, 28, 203 – 210.
- [45] Shah, R.K. Thermal entry length solutions for the circular tube and parallel plates. *Proceedings of 3rd National Heat and Mass Transfer Conf., Indian Institute of Technology, Bombay*. **1975**, Vol. I, 11-75.
- [46] Haghghi, E.B.; Anwar, Z.; Lumbreras, I.; Mirmohammadi, S.A.; Behi, M.; Khodabandeh, R.; Palm, B. Screening Single Phase Laminar Convective Heat Transfer of Nanofluids in a Micro-tube. *J. of Physics: Conference Series*. **2012**, 395, 012036.
- [47] Heris, S.Z.; Farzin, F.; Sardarabadi, H. Experimental comparison among thermal characteristics of three metal oxide nanoparticles/turbine oil-based nanofluids under laminar flow regime. *Int. J. Thermophys.* **2015**, 36, 760-782.
- [48] Bianco, V., Chiacchio, F., Manca, O., Nardini, S. Numerical investigation on nanofluids forced convection in circular tubes, *Applied Thermal Engineering*. **2009**
- [49] Behzadmehr, A., Saffar-Avval, M. Galanis, N. Prediction of turbulent forced convection of a nanofluid in a tube with uniform heat flux using a two-phase approach. *International Journal of Heat and Fluid Flow*, **2007**: 28(2), 211- 219.

- [50] Akbari, M., Galanis, N., Behzadmehr, A. Comparative analysis of single and two-phase models for CFD studies of nanofluid heat transfer, *International Journal of Thermal Sciences*, **2011**: 50(8), 1343-1354.
- [51] Namburu, P.K. Das, D.K., Tanguturi, K.M., Vajjha, R.S. Numerical study of turbulent flow and heat transfer characteristics of nanofluids considering variable properties, *International Journal of Thermal Sciences*. **2008**.
- [52] Ting, H.H., Hou, S.S. Numerical study of laminar flow forced convection of water-Al<sub>2</sub>O<sub>3</sub> nanofluids under constant wall temperature condition, *Mathematical Problems in Engineering*. **2015**, 1-8.
- [53] Fard, M.H., Esfahany, M.N., Talaie, M.R. Numerical study of convective heat transfer of nanofluids in a circular tube two-phase model versus single-phase model, *International Communications in Heat and Mass Transfer*, Volume 37, Issue 1 (**2010**), 91-97.
- [54] Arzani, H.K., Arzani, H.K., Kazi, S.N., Badarudin, A. Numerical Study of Developing Laminar Forced Convection Flow of Water/CuO Nanofluid in a Circular Tube with a 180 Degrees Curvature, *International Journal of Chemical, Molecular, Nuclear, Materials and Metallurgical Engineering Vol:100, No:5*, **2016**.
- [55] Obot, N.T., Toward a better understanding of friction and heat/mass transfer in microchannels – a literature review. *Microscale Thermophysical Engineering*. **2003**, 6, 155-173.
- [56] Vafaei, S., Wen. D. Convective heat transfer of alumina nanofluids in a microchannel. *Proceedings of the 14<sup>th</sup> International Heat Transfer Conference*. **2010**.
- [57] Lee, J., Gharagozloo, P. E. Kolade, B. Eaton, J.K., Goodson. K. E. Nanofluid convection in microtubes. *Journal of Heat Transfer*. **2010**, 132 (9): 092401.
- [58] Heris, S.Z., Nassan, S.H. Noie, H., Sardarabadi, H., Sardarabadi, M. Laminar convective heat transfer of Al<sub>2</sub>O<sub>3</sub>/water nanofluid through square cross-sectional duct. *International Journal of Heat and Fluid Flow*. **2013**, 44:375-382.
- [59] Heyhat, M.M., Kowsary, F., Rashidi, A.M., Esfehiani, S.A.V., Amrollahi, A. Experimental investigation of turbulent flow and convective heat transfer characteristics of alumina water nanofluids in fully developed flow regime. *International Communications in Heat and Mass Transfer*. **2012**, 39:1272-1278.
- [60] Daungthongsuk, W., Wongwises, S. A critical review of convective heat transfer of nanofluids. *Renewable and Sustainable Energy Reviews*. **2007**, 11, 797-817.
- [61] Sundén, B. *Introduction to Heat Transfer*. Southampton: WIT Press. **2012**.
- [62] Dalkilic, S., Kayaci, N., Celen, A., Tabatabaei, M., Yildiz, O., Daungthongsuk, w., and S. wongwises. 2012. Forced convective heat transfer of nanofluids—A review of the recent literature. *Curr. Nanosci.* 8(6): 949–969.
- [63] Hussein, A. M., Sharma, K. V., Bakar, R. A., and K. Kadrigama. A review of forced convection heat transfer enhancement and hydrodynamic characteristics of a nanofluid. *Renew. Sust. Energy Rev.* **2014**, 29: 734–743.
- [64] Yang, C., Li, w., Sano, Y., Mochizuki, M., and A. Nakayama. On the anomalous convective heat transfer enhancement in nanofluids: A theoretical answer to the nanofluids controversy. *ASME J. Heat Transf.* **2013**, 135(5): 054504.
- [65] Humnic, G., and A. Humnic. Application of nanofluids in heat exchangers: A review. *Renew. Sust. Energy Rev.* **2012**, 16(8): 5625–5638.



- [66] Escher, W., Brunschwiler, T., Shalkevich, N., Shalkevich, A., Burgi, T., Michel, B., and Poulikakos, D. On the cooling of electronics with nanofluids. *ASME J. Heat Transf.* **2011**, 133(5): 051401.
- [67] Seyf, H. R., and Mohammadian, S.K. Thermal and hydraulic performance of counterflow microchannel heat exchangers with and without nanofluids. *ASME J. Heat Transf.* **2011**, 133(8): 081801.
- [68] Jang, S.P. and Choi, S.U. Free convection in a rectangular cavity (Bernard convection) with nanofluids, in: *Proceedings of the 2004 ASME International Mechanical Engineering Congress and Exposition, Anaheim, California, November 13-20, 2004.*
- [69] Gosselin, L., da Silva A.K. Combined heat transfer and power dissipation optimization of nanofluid flows, *Appl. Phys, Lett.* 85 (**2004**) 4160.
- [70] Lee, J., Mudawar, I. Assessment of the effectiveness of nanofluids for single-phase and two-phase heat transfer in micro-channels, *Int. J. Heat Mass Transfer* 50 (**2007**) 452-463.
- [71] Zhou, Sheng-Qi and Rui Ni. Measurement of the specific heat capacity of water-based Al<sub>2</sub>O<sub>3</sub> nanofluid, *Applied Physics Letters* 92, 093123 (**2008**).
- [72] Nguyen, C.T., Desgranges, F. Roy, G. Galanis, N., Mare, T., Boucher, S., Mints, H.A. Temperature and particle-size dependent viscosity data for water based nanofluids-hysteresis phenomenon, *Int. J. Heat Fluid Flow* 28 (**2007**) 1492 – 1506.
- [73] Akoh, H., Tsukasaki, Y., Yatsuya, S., Tasaki, A. Magnetic properties of ferromagnetic ultrafine particles prepared by vacuum evaporation on running oil substrate, *Journal of Crystal Growth* 45 (**1978**) 495–500.
- [74] Wagener, M., Murty, B.S., Gunther, B. Preparation of metal nanosuspensions by high-pressure DC-sputtering on running liquids, in: S. Komarneni, J.C. Parker, H.J. Wollenberger (Eds.), *Nanocrystalline and Nanocomposite Materials II*, vol. 457, Materials Research Society, Pittsburgh, PA, **1997**, pp. 149–154.
- [75] Eastman, J.A., Choi, U.S., Li, S., Thompson, L.J., Lee, S. Enhanced thermal conductivity through the development of nanofluids, *Materials Research Society Symposium – Proceedings*, vol. 457, Materials Research Society, Pittsburgh, PA, USA, Boston, MA, USA, **1997**, pp. 3–11.
- [76] Zhu, H., Lin, Y., Yin, Y. A novel one-step chemical method for preparation of copper nanofluids, *Journal of Colloid and Interface Science* 227 (**2004**) 100–103.
- [77] Lo, C.-H., Tsung, T.-T., Chen, L.-C. Shape-controlled synthesis of Cubased nanofluid using submerged arc nanoparticle synthesis system (SANSS), *Journal of Crystal Growth* 277 (1–4) (**2005**) 636–642.
- [78] Lee, S., Choi, S.U.S., Li, S., Eastman, J.A. Measuring thermal conductivity of fluids containing oxide nanoparticles, *Journal of Heat Transfer* 121 (**1999**) 280–289.
- [79] Wang, X., Xu, X., Choi, S.U.S. Thermal conductivity of nanoparticle–fluid mixture, *Journal of Thermophysics and Heat Transfer* 13 (4) (**1999**) 474– 480.
- [80] Murshed, M.S., Leong, K.C., Yang, C. Enhanced thermal conductivity of TiO<sub>2</sub>–water based nanofluids, *International Journal of Thermal Sciences* 44 (4) (**2005**) 367–373.
- [81] Xuan, Y., Li, Q. Heat transfer enhancement of nanofluids, *International Journal of Heat and Fluid Transfer* 21 (**2000**) 58–64.

- [82] Hwang, Y.J., Ahn, Y.C., Shin, H.S., Lee, C.G., Kim, G.T., Park, H.S., Lee, J.K. Investigation on characteristics of thermal conductivity enhancement of nanofluids, *Current Applied Physics*, in press.
- [83] Kreith, F., and M. S. Bohn. *Principles of Heat Transfer*, 5th ed. Boston, MA: PWS Publishing Company. **1997**.
- [84] Timofeeva, E. V. "Nanofluids for heat transfer—Potential and engineering strategies." In *Two Phase Flow, Phase Change and Numerical Modeling*, edited by A. Ahsan. Rijeka, Croatia: InTech, **2011**, 435–450.